



Disrupting the ArcA Regulatory Network Amplifies the Fitness Cost of Tetracycline Resistance in *Escherichia coli*

[®] Mario L. Arrieta-Ortiz, Min Pan, Amardeep Kaur, Evan Pepper-Tunick, Divek Srinivas, Ananya Dash, Ananya Dash, Ananya Christinal Immanuel, Anaron N. Brooks, Tyson R. Shepherd,
[®] Nitin S. Baliga Abde, Ananya Dash, An

^aInstitute for Systems Biology, Seattle, Washington, USA

^bMolecular Engineering Sciences Institute, University of Washington, Seattle, Washington, USA

cInscripta Inc, Boulder, Colorado, USA

^dDepartment of Biology, University of Washington, Seattle, Washington, USA

^eMolecular and Cellular Biology Program, University of Washington, Seattle, Washington, USA

fLawrence Berkeley National Lab, Berkeley, California, USA

⁹Department of Microbiology, University of Washington, Seattle Washington, USA

ABSTRACT There is an urgent need for strategies to discover secondary drugs to prevent or disrupt antimicrobial resistance (AMR), which is causing >700,000 deaths annually. Here, we demonstrate that tetracycline-resistant (Tet^R) Escherichia coli undergoes global transcriptional and metabolic remodeling, including downregulation of tricarboxylic acid cycle and disruption of redox homeostasis, to support consumption of the proton motive force for tetracycline efflux. Using a pooled genome-wide library of single-gene deletion strains, at least 308 genes, including four transcriptional regulators identified by our network analysis, were confirmed as essential for restoring the fitness of TetR E. coli during treatment with tetracycline. Targeted knockout of ArcA, identified by network analysis as a master regulator of this new compensatory physiological state, significantly compromised fitness of Tet^R E. coli during tetracycline treatment. A drug, sertraline, which generated a similar metabolome profile as the arcA knockout strain, also resensitized TetR E. coli to tetracycline. We discovered that the potentiating effect of sertraline was eliminated upon knocking out arcA, demonstrating that the mechanism of potential synergy was through action of sertraline on the tetracycline-induced ArcA network in the Tet^R strain. Our findings demonstrate that therapies that target mechanistic drivers of compensatory physiological states could resensitize AMR pathogens to lost antibiotics.

IMPORTANCE Antimicrobial resistance (AMR) is projected to be the cause of >10 million deaths annually by 2050. While efforts to find new potent antibiotics are effective, they are expensive and outpaced by the rate at which new resistant strains emerge. There is desperate need for a rational approach to accelerate the discovery of drugs and drug combinations that effectively clear AMR pathogens and even prevent the emergence of new resistant strains. Using tetracycline-resistant (Tet^R) *Escherichia coli*, we demonstrate that gaining resistance is accompanied by loss of fitness, which is restored by compensatory physiological changes. We demonstrate that transcriptional regulators of the compensatory physiologic state are promising drug targets because their disruption increases the susceptibility of Tet^R *E. coli* to tetracycline. Thus, we describe a generalizable systems biology approach to identify new vulnerabilities within AMR strains to rationally accelerate the discovery of therapeutics that extend the life span of existing antibiotics.

KEYWORDS ArcA, *Escherichia coli*, antibiotic resistance, compensatory mechanism, global regulatory networks, systems biology, tetracycline

Editor Pedro H. Oliveira, Génomique Métabolique, Genoscope, Institut François Jacob, CEA, CNRS, Université d'Évry, Université Paris-Saclav

Copyright © 2022 Arrieta-Ortiz et al. This is an open-access article distributed under the terms of the Creative Commons Attribution 4.0 International license.

Address correspondence to Nitin S. Baliga, nbaliga@isbscience.org.

*Present address: Ananya Dash, Emory University, Georgia, USA.

The authors declare a conflict of interest. Aaron N. Brooks and Tyson R. Shepherd are affiliated with Inscripta Inc. Inscripta Inc contributed reagents for this study.

Received 23 September 2022 Accepted 9 November 2022 Published 20 December 2022 ntimicrobial resistance (AMR) is the ability of a bacterium to withstand growth inhibition and killing by high doses of an antibiotic (1, 2). The problem of AMR has emerged from the overprescription and overuse of antibiotics (3–5), accumulation of antibiotics in the natural environment (6), antibiotic-induced increased mutation rates (7, 8), horizontal transfer of resistance-conferring genes (3), and poor infection-control strategies (9). As a result, infections by pathogenic AMR strains are rapidly growing and projected to cause \sim 10 million deaths/year by 2050 (4). Sadly, consistent with this prediction, \sim 5 million deaths in 2019 were associated with infections caused by AMR strains of bacterial pathogens (10). While health policies to regulate antibiotic use (11) and programs to ensure patient compliance with completing prescribed antibiotic regimens are effective (12), these efforts are expensive, laborious, and face implementation challenges around the world (13). Similarly, efforts to find new potent antibiotics are effective (14) but also expensive and being outpaced by the rate at which new resistant strains are emerging (15).

A solution to tackling AMR might be in the observation that gaining resistance to an antibiotic is typically associated with loss of fitness (3), which can be restored through compensatory mutations (3) that cause changes in regulation and metabolism (16–18). For example, *Pseudomonas aeruginosa* upregulates anaerobic nitrate respiration to quench intracellular protons and compensate for loss of fitness due to efflux-mediated resistance (19). Similarly, Mycobacterium smegmatis transcriptionally upregulates the rRNA methylase TlyA to restore fitness upon gaining resistance to capreomycin (20). Molecules that target new vulnerabilities within compensatory mechanisms of antibiotic resistance could enable the recovery of "lost" antibiotics and broaden the life span of new antibiotics (21, 22). The ability of metabolite supplementation to resensitize resistant pathogens to diverse antibiotics, including aminoglycosides (23), chloramphenicol, and streptomycin (24), lends credibility to this idea. However, to implement such a strategy at scale, we need to develop methodology to discover the mechanistic driver(s) of fitness-restoring compensatory changes in AMR strains, confirm with targeted genetic perturbations that these mechanistic drivers do indeed represent new vulnerabilities, and use a rational approach to find molecules that could disrupt the compensatory mechanism (25).

Here, we have developed a systems approach to discover and target mechanistic drivers of the compensatory physiologic state of tetracycline-resistant (here called Tet^R) *Escherichia coli*. Discovered in 1947, tetracyclines are protein synthesis inhibitors that act by binding to the 30S ribosomal subunit (26, 27). Tetracyclines were rapidly adopted in the clinic due to their broad spectrum efficacy (26, 27) and continue to be used widely in animal farming (28). Resistance to tetracyclines emerged a few years later in 1953 and progressively reduced their effectiveness (26, 27). The primary mechanisms of tetracycline resistance are (i) through active extrusion by efflux pumps; (ii) gain of mutations that disrupt interaction with the target; and (iii) enzymatic inactivation, e.g., by TetX (26, 27). Previous attempts to counteract tetracycline resistance in *E. coli* have focused on potential efflux pump inhibitors (29, 30).

We have discovered that when *E. coli* gains resistance to tetracycline through AcrAB-mediated efflux, a global shift in metabolism to a fermentative state is required to restore fitness of the resistant strain in the presence of tetracycline. The regulatory network that mechanistically drives this global metabolic reprogramming in the Tet^R strain is comprised of at least 25 transcription factors (TFs) that directly regulate 279 genes. Interestingly, 209 of the 279 genes are differentially regulated by 15 TFs in the presence of tetracycline, suggesting that increased activity of the AcrAB efflux pump causally alters the activity of these regulators. Using a pooled barcoded library of CRISPR-generated knockout strains, we performed a genome-wide fitness screen that uncovered 308 genes essential for restoring fitness of Tet^R *E. coli* during treatment with tetracycline. In fact, the fitness screen validated mechanistic predictions from our network-based strategy that four TFs (ArcA, CytR, PhoP, and RpoS) contributed to the compensatory physiologic state required for restoring the fitness of Tet^R *E. coli* in the

presence of tetracycline. Further, the fitness screen also confirmed that, as predicted, tetracycline treatment drove Tet^R *E. coli* from aerobic respiration toward a fermentative physiologic state. Targeted knockout of *arcA*, a master regulator of this network, further confirmed its role in restoring fitness of the Tet^R strain. We discovered that the drug sertraline, which generated a similar metabolome profile as the *arcA* knockout, potentiated the bacteriostatic effect of tetracycline on the Tet^R strain, but not the wild-type strain, on which the effect was additive. We also show that deleting *arcA* abolished the potentiating effect of sertraline, demonstrating that the mechanism of its potential synergy with tetracycline was through its action on the tetracycline-induced and ArcA-regulated network. We discuss these results from the perspective of formulating a multidrug regimen using a network-based approach to recover lost antibiotics and prolong the utility of new antibiotics.

RESULTS

A novel physiological state underlies tetracycline resistance in *E. coli*. To identify mutations that may contribute to the tetracycline resistance phenotype of Tet^R *E. coli*, we resequenced and compared the genomes of the tetracycline-susceptible wild-type (MG1655, here called "WT") and laboratory-evolved Tet^R strains of *E. coli* (31, 32). We discovered that gaining tetracycline resistance could be due to mutations in *acrB* and *acrR* genes, which were independently reported by Hoeksema et al. (33) (complete list of mutations shown in Table S1). AcrR is a transcriptional repressor of the *acrAB* operon, and mutations in this gene are consistent with upregulation of the efflux pump (see below) (33). Interestingly, we also identified an in-frame deletion in *mlaA*, which encodes a component of the system for maintenance of lipid asymmetry (34). He et al. have recently associated this deletion in the *mlaA* gene with resistance to tigecycline (a glycylcycline, a tetracycline derivative [35]), even in the absence of *acrAB* (36). Thus, multiple mechanisms may simultaneously contribute to the resistance phenotype.

To characterize direct and compensatory physiological changes triggered by the acquisition of antibiotic resistance, we also reanalyzed transcriptomes of the TetR and WT strains with and without tetracycline treatment (32). In the absence of tetracycline, the Tet^R strain differentially expressed 197 genes (DEGs; adjusted *P* value < 0.05 and absolute log₂ fold change >1) relative to the WT strain, including 65 metabolic genes, seven transcription factors (TFs) and four efflux pump (EP)-related genes (including the acrAB operon) (Fig. 1A). Functional enrichment on the dysregulated gene set revealed that 13 functional terms were significantly perturbed in the Tet^R strain (Fig. 1B; Table S2). Of note was differential regulation of 33 fermentation-related genes (randomized permutation test P value < 0.01), including the frd operon, adhE, fumC, and IdhA (which had P value < 0.05) (Fig. S1). Notably, upregulation of the acrAB operon and acrZ was consistent with known mechanisms of resistance to tetracycline and other antibiotics (Fig. S2A) (30, 37, 38). Disruption of the AcrAB efflux pump has been demonstrated to reduce the MIC of tetracycline to 0.5 μ g/mL, which was 4-fold lower than for wild-type E. coli K-12 (reported as 2 μ g/mL) (30), and also the overall fitness in the presence of tetracycline (39) (Fig. S2B).

The Tet^R strain differentially expressed nearly 10 times as many genes as the WT (with 896 versus 93 DEGs) in response to treatment with 0.25 and 16 μ g/mL of tetracy-cline for WT and Tet^R, respectively (Fig. 1A) (32). This differential regulation represented reprogramming of multiple processes (based on enrichment of 67 functional terms per the hypergeometric test), including the tricarboxylic acid (TCA) cycle (15 of 21 genes; P value = 1.7e-6), the electron transport chain (ETC, 13 of 23 genes; P value = 3.2e-4), and ATP synthase (four of eight genes; P value = 0.076) (Fig. 1B and C; Table S2). While tetracycline treatment did not result in substantial upregulation of the acrAB efflux pump in the Tet^R strain (i.e., variation in $acrAB \log_2$ fold change was less than 0.35; Fig. S2A), it induced the upregulation of at least four additional efflux pump genes (Fig. 1A). This suggested that the large-scale transcriptional remodeling, which was potentially mediated by 35 differentially expressed TFs (Fig. 1), might constitute

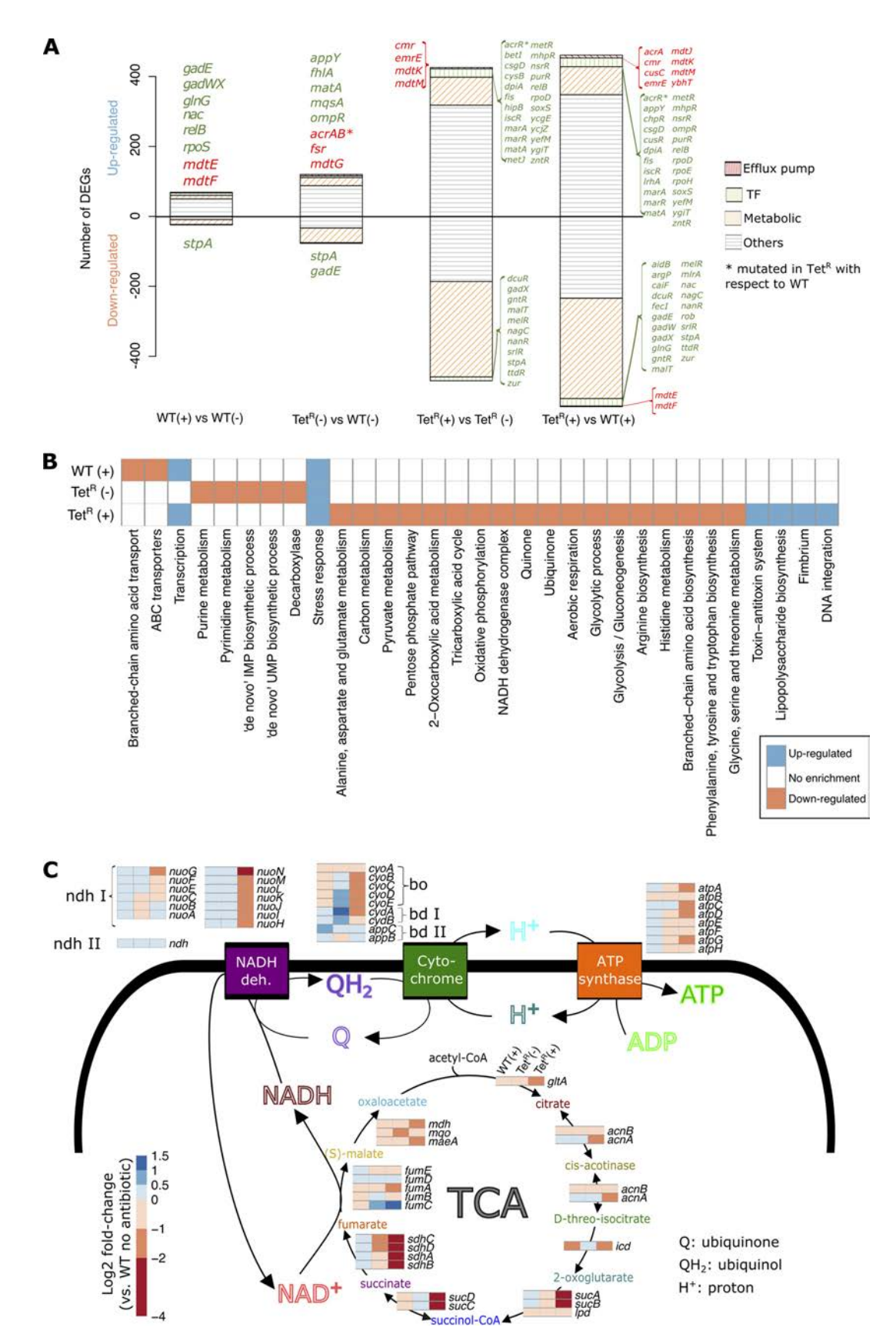


FIG 1 Transcriptional and metabolic remodeling accompanying gain of tetracycline resistance in *E. coli*. (A) Comparison of transcriptomes of Tet^R and parental WT (MG1655) strains in the presence (+) and absence of tetracycline (-). Tetracycline concentrations used for wild-type (WT) and Tet^R strains (Continued on next page)

a compensatory physiologic state that is triggered by increased efflux pump activity in the presence of tetracycline to ameliorate the loss of fitness associated with the resistance phenotype of the TetR strain (i.e., maximum growth rate and area under the growth curve of the TetR strain were \sim 30% lower than the corresponding fitness estimates of the WT strain; see below) (3). Specifically, repression of aerobic oxidative phosphorylation and induction of fermentation pathways suggested that a shift toward an anoxic physiologic state might be necessary to support the tetracycline resistance phenotype.

A transcriptional program governed by 25 TFs underlies the physiological state required for tetracycline resistance. We analyzed gene expression changes induced by gain of tetracycline resistance in the context of the transcriptional regulatory network to discover mechanisms responsible for regulatory and metabolic reprogramming of the Tet^R strain. We compiled a signed transcriptional regulatory network of E. coli based on curated positive or negative attributes to every TF-target gene interaction in RegulonDB (40). We then used the NetSurgeon algorithm (41) to identify within this transcriptional regulatory network the subset of TFs whose simulated overexpression and knockout explained the overall gene expression changes induced by gain of mutations (e.g., the acrR mutation) and treatment with tetracycline in the Tet^R strain. We hypothesized that the TF networks that were differentially active in the Tet^R strain upon tetracycline treatment were likely to be the mechanistic drivers of the compensatory physiologic state that was needed to support the resistance phenotype. Altogether, the NetSurgeon-based analysis implicated 25 TFs in mechanistically driving the differential regulation of 279 genes in the Tet^R strain, of which 209 genes were regulated by a subset of 15 TFs in response to tetracycline treatment (Table 1). Of the 25 TFs, 17 were part of two TF-TF network modules, suggesting coordination across their regulatory networks (Fig. 2A). While one subnetwork included TFs that were previously linked to AMR (MarA, SoxS, and Rob) (42), the other subnetwork was made up of TFs that control metabolic pathways (Lrp, MalT, GatR, and ArcA).

In a second independent approach, we used network component analysis to estimate the differential regulatory activity of TFs in Tet^R and WT with and without tetracy-cline treatment (43) (see Materials and Methods). The estimated regulatory activities of TFs were consistent with NetSurgeon predictions for 12 of the 25 TFs (indicated with brown node border in Fig. 2A). Finally, in a third approach, we discovered that 287 DEGs were statistically over-represented across 29 gene modules regulated by 15 (of the 25 TFs) within the previously developed Environment and Gene Regulatory Influence Network (EGRIN) model for *E. coli* (44). In summary, of the 25 TFs identified by NetSurgeon, 7 were also identified by the 2 orthogonal approaches. Altogether, the 15 TFs implicated in the response of Tet^R to tetracycline collectively regulated 23.3% (209 genes, hypergeometric test *P* value < 1e-26) of all DEGs, including 6 additional TFs, explaining how the response might have propagated to other genes in the genome. Notably, the predicted increased and decreased activity of TFs were consistent with the changes in expression profiles of their corresponding regulons across strains and treatments (Fig. 2B).

ArcA, a global transcriptional regulator that is typically induced under microaerobic conditions (45), was implicated by all three approaches as a mechanistic driver of the tetracycline response in the Tet^R strain. ArcA is a master regulator of one of the two TF-

FIG 1 Legend (Continued)

were 0.25 and 16 μ g/mL, respectively. Transcriptomics data were sourced from Händel et al. (32). Differentially expressed genes (adjusted *P* value < 0.05 and absolute \log_2 fold change > 1) were classified as efflux pump-related (compiled from the EcoCyc database and available literature) (53, 102), transcription factors (TFs) (based on the transcriptional regulatory network compiled from the RegulonDB database), or metabolism-related (based on the iJO1366 metabolic model of *E. coli*) (40, 102, 103). Unassigned genes were grouped in the "Others" category. Differentially expressed TFs and efflux pump genes are listed in green and red type, respectively. (B) Heat map with functional enrichment information of the set of genes significantly up- and downregulated in the WT strain in the presence of tetracycline and the Tet^R strain without and with tetracycline with respect to the WT strain in antibiotic-free condition. Due to space constraints and functional terms redundancy, only a subset of functional terms are displayed (full list on Table S2). (C) Fold change profiles (with respect to the WT strain in antibiotic free condition) of genes related to the tricarboxylic acid (TCA) cycle, the electron transport chain (i.e., NADH dehydrogenases [NADH deh.], and cytochromes), and ATP synthase. Pathways of interest and associated genes were compiled from the EcoCyc database (102) and available literature (104). DEG, differentially expressed gene.

TABLE 1 TFs implicated in reprogramming transcriptional response of the Tet^R strain^a

| Transcription | Locus tag | Differential activity ^b | Response ^c | Regulon size ^d | Targets | |
|---------------|--------------|------------------------------------|-----------------------|---------------------------|---------|-----------------------|
| factor | | | | | Basale | Adaptive ^f |
| RpoS | b2741 | Decreased | Adaptive | 207 | 20 | 69 |
| ArcA | b4401 | Increased | Adaptive | 167 | 9 | 66 |
| HNS | b1237 | Decreased | Basal | 146 | 18 | 33 |
| Cra (FruR) | b0080 | Increased | Adaptive | 76 | 2 | 43 |
| Lrp | b0889 | Increased | Both | 64 | 9 | 32 |
| PhoP | b1130 | Decreased | Basal | 49 | 9 | 15 |
| GadE | b3512 | Decreased | Both | 36 | 9 | 14 |
| SoxS | b4062 | Increased | Basal | 33 | 7 | 13 |
| MarA | b1531 | Increased | Basal | 33 | 11 | 11 |
| RcsB | b2217 | Decreased | Basal | 33 | 7 | 10 |
| PurR | b1658 | Increased | Basal | 31 | 10 | 10 |
| Rob | b4396 | Increased | Basal | 22 | 8 | 7 |
| FliZ | b1921 | Increased | Basal | 20 | 6 | 6 |
| CytR | b3934 | Increased | Adaptive | 13 | 0 | 8 |
| OmpR | b3405 | Increased | Both | 13 | 4 | 6 |
| TorR | b0995 | Decreased | Basal | 12 | 3 | 4 |
| MalT | b3418 | Decreased | Adaptive | 10 | 0 | 8 |
| DgsA | b1594 | Increased | Adaptive | 10 | 0 | 7 |
| NrdR | b0413 | Decreased | Adaptive | 9 | 1 | 4 |
| AdiY | b4116 | Decreased | Both | 8 | 3 | 5 |
| YbjK | b0846 | Increased | Adaptive | 8 | 1 | 5 |
| PspF | b1303 | Increased | Both | 7 | 4 | 5 |
| GatR | b4498 | Increased | Adaptive | 6 | 0 | 6 |
| GlcC | b2980 | Increased | Basal | 6 | 3 | 3 |
| BirA | b3973 | Decreased | Adaptive | 5 | 0 | 5 |

^aDEG, differentially expressed gene; TF, transcription factor.

TF subnetworks, directly regulating 66 DEGs and influencing regulation by at least four downstream TFs (Fig. 2A; Table 1). There was significant overlap between DEGs in the Tet^R response to tetracycline and DEGs in an arcA deletion strain in anaerobic conditions (46) (hypergeometric test P value <1e-11). Importantly, ArcA is a known repressor of most genes of the TCA cycle and ETC (47) (Fig. 2A), and both processes were significantly downregulated in the Tet^R strain in the presence of tetracycline, which could have potentially perturbed NADH/NAD ratio and disrupted energy production via aerobic respiration. ArcA directly coordinates repression of the TCA cycle with activation of overflow metabolism (48), which is a fermentation mechanism to generate energy, albeit at lower efficiency, to cope with changes in demand for protein, energy, and biomass production under changing growth conditions (49, 50). Interestingly, fermentation genes were expressed at a higher level in the Tet^R strain even without tetracycline treatment, although the expression of TCA genes was downregulated only in the presence of tetracycline (Fig. 1C; Fig. S1). Based on these observations, we hypothesized that fitness loss associated with gain of efflux-mediated resistance to tetracycline in the Tet^R strain is compensated by an ArcA-mediated shift toward energy production by fermentation (48).

Genome-wide CRISPR screen corroborates network-predicted mechanisms underlying a compensatory physiologic state that supports tetracycline resistance. We investigated how each gene in the *E. coli* genome contributed to the compensatory physiologic state required to support the tetracycline resistance phenotype by performing an unbiased genome-wide CRISPR knockout (KO) screen. In brief, we constructed

b"Increased" and "Decreased" indicate NetSurgeon-inferred change in the activity of each TF that explains the observed transcriptional response in a given treatment.

c"Basal" indicates the role of a TF in reprogramming transcriptional response of the Tet^R strain in the absence of tetracycline, whereas "Adaptive" indicates that the TF mediates transcriptional response of the Tet^R strain to tetracycline.

^dTotal number of genes directly regulated by each TF.

 $^{^{\}it e}$ Number of DEGs regulated by a TF in the absence of tetracycline.

 $^{{}^}f\!\text{Number}$ of DEGs regulated by a TF in the presence of tetracycline.

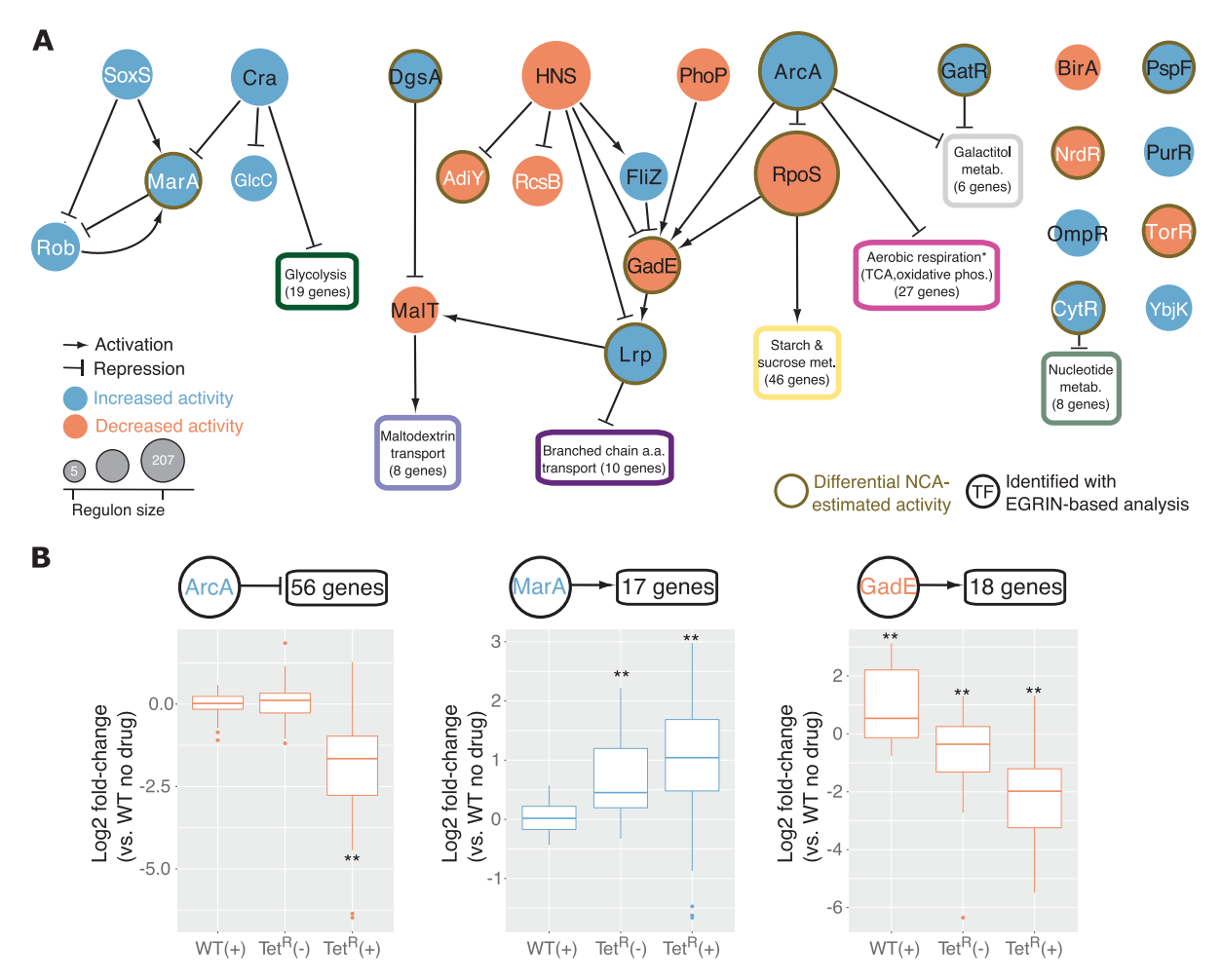


FIG 2 Regulatory circuits differentially active in tetracycline-resistant E. coli. (A) Subnetwork of 25 TFs (displayed as circles) implicated in driving transcriptional and metabolic reprogramming in the Tet^R strain (Table 1). TF autoregulation is not displayed. Functional enrichment (due to space constraints, only the functional term with the lowest P value is displayed) within subsets of six or more genes differentially expressed during Tet^R response to tetracycline and regulated by the same TF(s) implicated in Tet^R adaptive state (Table 1) are shown within boxes. The numbers in parentheses indicate the number of genes used to perform the functional enrichment analyses with DAVID (91) (not all genes may be associated with the shown functional term). The asterisk (*) indicates that the term was manually defined taking into account the overlap among multiple over-represented terms. TFs implicated by network component analysis (NCA) in regulatory and metabolic reprogramming of the Tet^R strain are indicated in nodes with a brown-colored border. Black font indicates TFs that were implicated based on significant overlap of their differentially regulated targets (in the Tet[®] background) within coregulated gene modules in EGRIN (Environment and Gene Regulatory Influence Network) (44). The network was visualized using Cytoscape version 3.4.0 (105). (B) Fold change of the ArcA, MarA, and GadE regulons (transcriptional data from Händel et al. [32]) support their predicted increased (for ArcA and MarA) and decreased (for GadE) activity in mediating transcriptional reprogramming of the Tet^R strain at baseline and during adaptive response to tetracycline treatment. For dual regulators (i.e., activating and repressing different genes), the regulatory activity on the majority of their differentially expressed target genes (~80%) is shown. Boxplots display fold change of differentially expressed regulon members in the basal and/or adaptive states (number of regulated genes by each TF is indicated above each corresponding boxplot). Boxes cover the 25th and 75th percentile ranges. Horizontal lines in boxes indicate median values. Absence and presence of tetracycline treatment is indicated with "(-)" and "(+)," respectively. Statistical significance of the observed mean fold changes was evaluated by determining the null distribution of mean fold change in 10,000 random samplings of gene sets of similar size. P values are indicated with * (<0.05) and ** (<0.001).

genome-wide knockout libraries using the Onyx Digital Genome Engineering Platform. The KO library consisted of 8,271 mutants, representing approximately two knockout designs for each gene in the Tet^R and WT strain backgrounds. The libraries were independently grown in quadruplicate over three rounds of sequential growth cycles (t0 to t3) in batch cultures with and without tetracycline (see Materials and Methods for details). To track the relative abundance of each KO strain in the population throughout the experiment, we performed barcode sequencing of the starting cultures, as well as at the end of each cycle. To account for the compositional nature of the data, we quantified changes in barcode abundance as the interquartile log ratio (IQLR) using ALDEx2 (51).

This allowed us to compare the barcode abundance for each gene KO at each growth cycle relative to its starting abundance (t0) while controlling for changes in the overall library composition (Fig. 3A).

Comparing across strain backgrounds (Tet^R and WT) and treatments (+/- tetracy-cline), the ALDEx2 analysis revealed a multitude of context-dependent effects. In the presence of tetracycline, for example, KOs in 1,261 genes affected fitness in the Tet^R background compared to only 363 genes in the WT background (Data Set S1). Strikingly, we observed that KOs in 874 genes significantly improved fitness uniquely in the context of tetracycline treatment in the Tet^R strain background (Fig. S3A). Genes that were dispensable during tetracycline treatment in the Tet^R strain span a wide range of functions and processes, including iron homeostasis (17 genes), cell adhesion (21 genes), and aerobic metabolism (12 TCA-related genes and 7 ETC-related genes and *atpE*, which encodes a subunit of the ATP synthase) (Fig. S3B).

We also identified genes that became important for growth during tetracycline treatment, particularly in the Tet^R strain background. This finding was supported by two analyses: First, we observed many instances in which both KO designs for a gene were undetectable by the end of the experiment following treatment with tetracycline in the Tet^R background ("dropouts"; 82 genes in WT background compared to 726 genes in the Tet^R background [with 43 genes in common]) (Fig. 3A; Data Set S2). These 726 dropout genes included the AcrAB efflux pump-related genes acrB and acrR, both carrying SNPs in the Tet^R genome (Table S1), and the arcA and arcB genes, which encode the ArcB-ArcA two-component system (52). Translation-related genes encoding ribosomal subunits, ribosome biogenesis, and rRNA binding were also among the KOs not detected at the end of the experiment (Fig. 3B). Second, relative abundance analysis with ALDEx2, which accounted for potential compositional bias in strain abundance (see above), corroborated significant purifying selection of 308 single-gene KO strains during tetracycline treatment of the Tet^R strain. Within this group, 234 singlegene KO strains (including arcA) were under purifying selection only on the Tet^R strain (Fig. S3A). Gene sets identified by both analyses were significantly similar (hypergeometric test P value = 0.012). As expected, KOs identified with ALDEx2 as having a deleterious effect included genes associated with varied mechanisms of antimicrobial resistance, for example, acrZ, a component of the AcrAB efflux pump (37); mdtA, a member of a resistance-nodulation-division (RND) multidrug efflux pump (53); and uvrA, an excision repair system protein (Fig. 3C) (54, 55). Notably, a significant number of genes that contributed fitness to the Tet^R strain in the presence of tetracycline were associated with anaerobic respiration, and included menaguinone biosynthesis genes (menA, menB, menC, menE, and menH) (DAVID functional term adjusted P value = 5.8e-2) (Fig. S3B), fumarate reductase (frdB and frdC), anaerobic glycerol-3-phosphate dehydrogenase (glpC), selenate reductase (ynfF), formate dehydrogenase-N subunit (fdnH), hydrogenase 2 membrane subunit (hybB), and malate dehydrogenase (mdh) (56-63) (Fig. S4). Together with the transcriptome analysis, these results strongly suggest that a distinct anaerobic state supports tetracycline resistance in the Tet^R background.

To understand whether transcriptional regulatory mechanisms drive large-scale physiological remodeling in the Tet^R background, we analyzed the fitness effects of TFs in the high-throughput CRISPR KO screen. Fifteen TF KOs significantly reduced fitness in the Tet^R background, but, interestingly, only following tetracycline treatment (Fig. S3C). This finding underscores the importance of global transcriptional reprogramming for the tetracycline resistance phenotype in the Tet^R background (Fig. 1 and 2A). Reassuringly, there was a high degree of overlap between the CRISPR screen in the presence of tetracycline and our network-based approach (10 of 24 TFs identified by the network-based approach and with KO designs, including *arcA*, *cytR*, *phoP*, and *rpoS*) (Fig. 2A and 3C). Notably, *arcA* and *phoP* were among the most deleterious KOs in the CRISPR screen after the first growth cycle. Together, these findings suggest that the tetracycline resistance phenotype in Tet^R *E. coli* is associated with transcriptional coordination of fermentative carbon metabolism by ArcA, acid stress response by

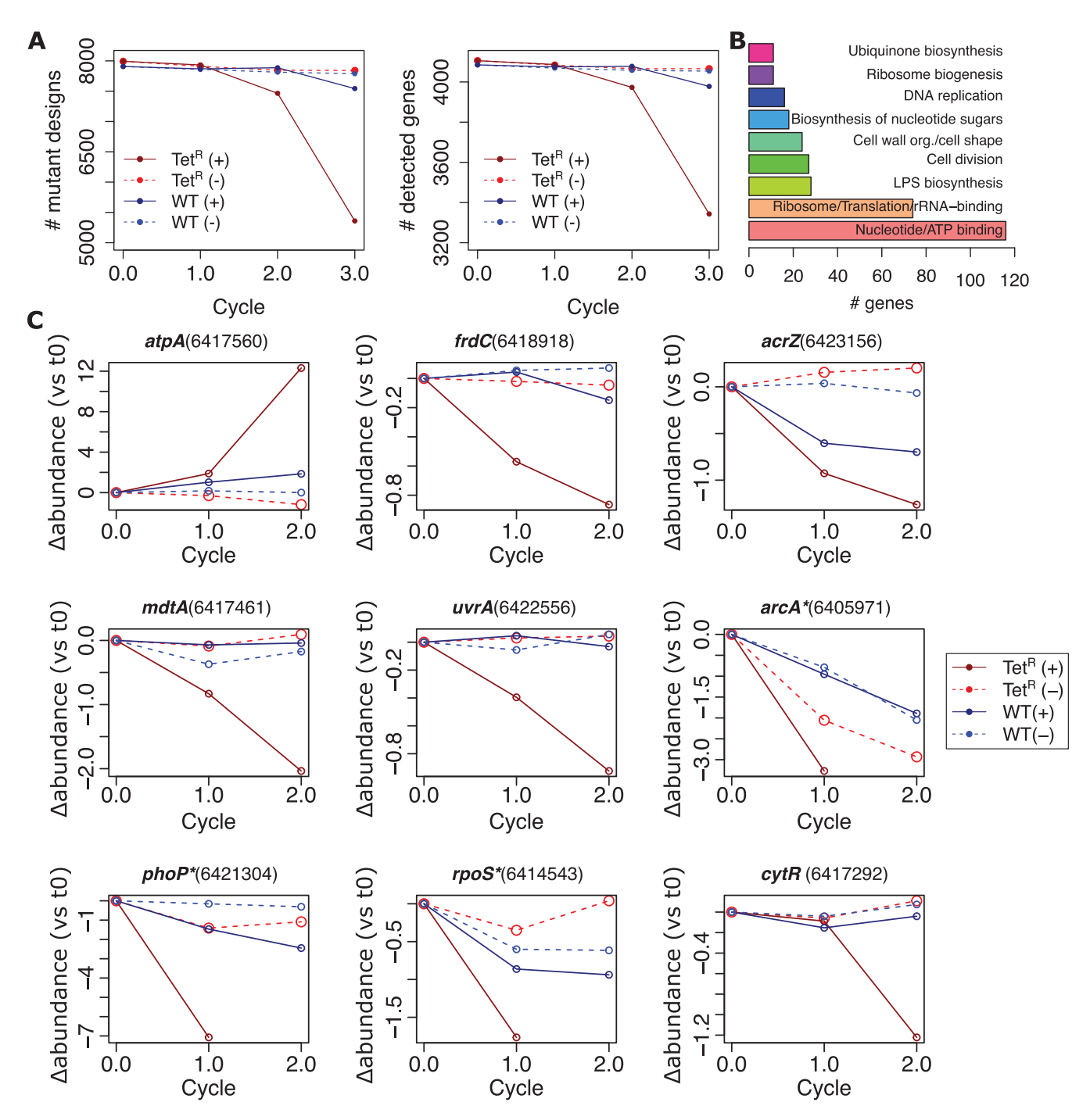


FIG 3 Gain of tetracycline resistance is associated with loss of robustness to genomic perturbations in the Tet^R strain. (A, left) Number of gene knockouts (KOs) detected during competitive growth assay in Tet^R and WT backgrounds with and without tetracycline treatment. Genome-wide KO libraries included on average two designs per gene, totaling 8,271 KOs. For a given time point, KOs that were not detected (i.e., <10 reads) in any of the four biological replicates were considered "dropouts." (Right) Aggregation by gene. Genes were considered undetected if both KO designs were dropouts. (B) General theme of functional term clusters identified by DAVID functional annotation clustering (91) in the set of 726 genes depleted in Tet^R due to tetracycline treatment at the end of the competition assay (t3). (C) Changes in ALDEx2 (51) estimated interquartile log ratio (IQLR) transformed relative abundance (each cycle normalized to the initial time point, t0) of selected KOs during growth assays of Tet^R and WT genome-wide single-gene deletion libraries. For each selected gene, the profile of difference in abundance (i.e., the "diff.btw" scores computed by ALDEx2) of a single design KO is shown (design ID indicated in parenthesis). KOs that were undetectable at t2 (<10 reads in any replicate) are indicated with an asterisk (*) next to the gene name. Relative abundance was not estimated for undetected designs. The absence and presence of tetracycline in the experiments are indicated with the "(-)" and "(+)" symbols next to the strain background labels, respectively. LPS, lipopolysaccharide.

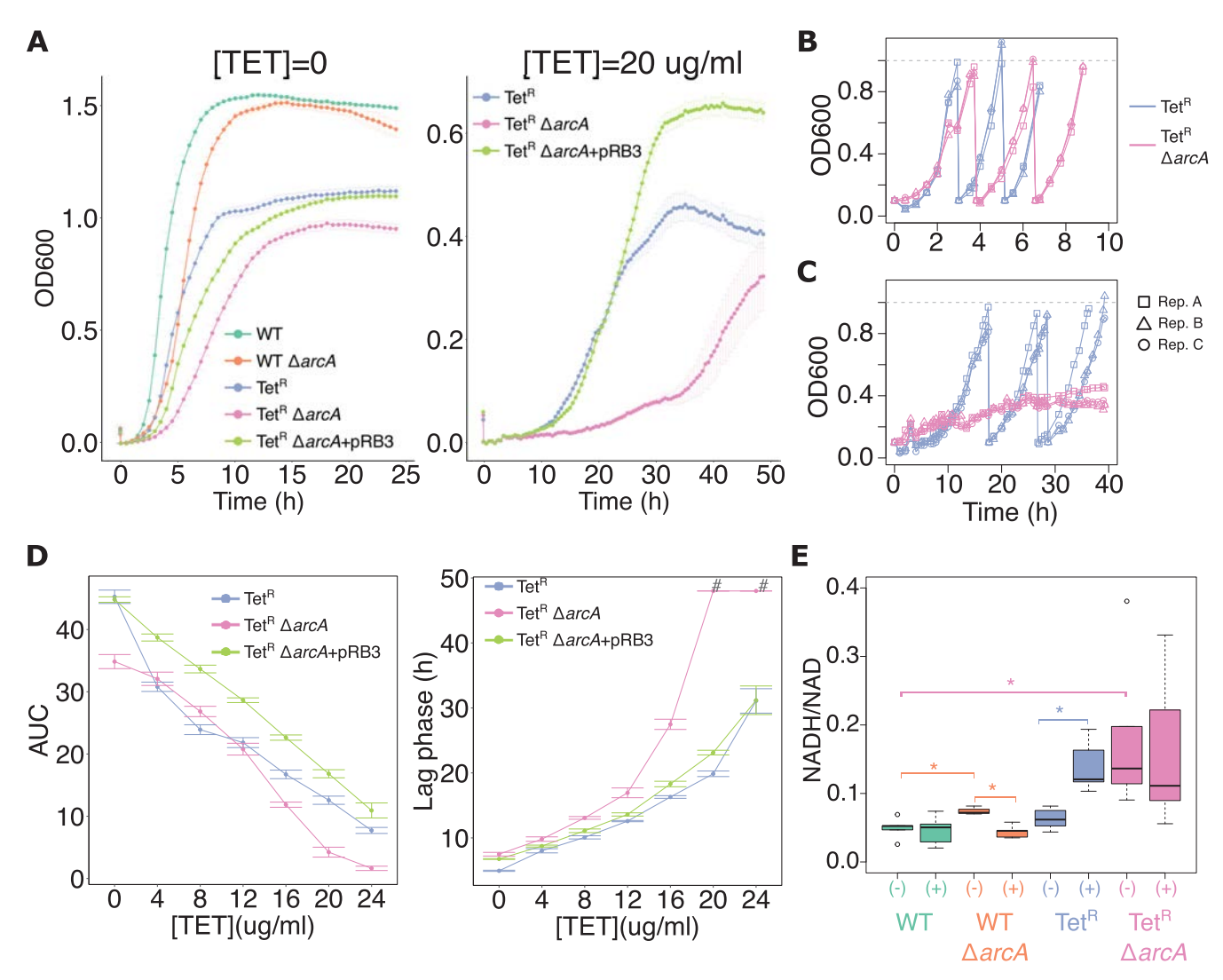


FIG 4 ArcA restores fitness of tetracycline-resistant *E. coli.* (A) Representative growth curves in LB medium for 48h with and without tetracycline (TET). Six replicates (Rep.) (i.e., three biological replicates with two replicates each) per strain were used. Points indicate average values and error bars indicate standard deviation. Effect of *arcA* deletion on Tet^R fitness in LB broth cultures without (B) or with 20 μg/mL of tetracycline (C) over three growth cycles is shown. In each cycle, cultures were started at an optical density at 600 nm (OD₆₀₀) of 0.1 and grown to an OD₆₀₀ of 1.0 (indicated by the gray dashed lines) and thereafter diluted in fresh medium to OD₆₀₀ of 0.1 to reinitiate a new cycle of growth. (D) Area under the growth curve (AUC) and lag phase (approximated by Growthcurver-estimated time of inflection, the time required to achieve half of maximal OD₆₀₀ [68]) for seven different concentrations of tetracycline. The # symbol indicates samples in which Growthcurver-estimated time of inflection was longer than the actual duration of the experiment and therefore adjusted to 48 h. (E) NADH/NAD ratio during log phase of the WT, WT Δ*arcA*, Tet^R, and Tet^R Δ*arcA* strains in the absence (indicated with "(+)") of tetracycline. NADH/NAD ratios in the absence of tetracycline were compared with respect to untreated WT using a Welch's *t* test. Similarly, ratios in the tetracycline-treated condition versus the untreated condition were compared for each strain; *P* values < 0.05 are indicated with the asterisk (*) symbol. Tet^R Δ*arcA*+pRB3, *arcA* deletion strain complemented with episomal copy of *arcA*.

PhoP (64), generalized stress response by RpoS (65), and carbon and nucleotide metabolism by CytR (66, 67) (Fig. 3C). These findings also implicate ArcA as a key TF that drives the physiological shift of the Tet^R strain to a fermentative state following treatment with tetracycline.

ArcA activity ameliorates the fitness cost of tetracycline resistance. We further investigated the importance of ArcA activity for tetracycline resistance by constructing an in-frame knockout ($\Delta arcA$) in the WT and Tet^R strain backgrounds and quantifying the overall fitness of both sets of parental and $\Delta arcA$ strains by calculating the area under the growth curve in batch cultures (68–70) (Fig. 4A to D). The fitness analysis demonstrated that gain of tetracycline resistance had significantly increased the relative importance of ArcA in the Tet^R strain (Fig. 4A), especially in the presence of high doses of tetracycline (16 to 24 μ g/mL). In fact, in the presence of tetracycline, the Tet^R

 $\Delta arcA$ strain was unable to achieve half the overall carrying capacity of the parental strain even after extended culturing (Fig. 4B and C). In stark contrast, the arcA deletion had a more subtle effect in the parental WT strain (Fig. S5). The fitness defect of the Tet^R $\Delta arcA$ strain during tetracycline treatment was completely reversed upon complementation with an episomal copy of arcA (Fig. 4D).

It has been demonstrated that increase in intracellular NADH/NAD ratio, such as during fast growth (49), triggers ArcA (71, 72), which then mediates repression of the TCA cycle and activation of overflow metabolism to prevent further redox imbalance (49). Consistent with this sequence of events, we observed that tetracycline treatment significantly increased the intracellular NADH/NAD ratio in the Tet^R strain, which explains the increased activity of ArcA with gain of tetracycline resistance (Fig. 4E). As expected, deletion of *arcA* resulted in constitutive dysregulation of NADH/NAD ratio irrespective of tetracycline treatment, presumably due to disruption of the ArcA-mediated feedback mechanism to manage redox balance (Fig. 4E). We propose based on these results that ArcA plays a central role in modulating redox balance to support increased efflux-mediated tetracycline resistance phenotype.

Molecules that mimic ArcA knockout phenotype disrupt efflux-mediated tetracycline resistance. In order to identify drugs that would simulate an arcA knockout phenotype, we leveraged available comparisons of metabolome profiles of drugtreated and single-gene deletion strains of E. coli (25). Among the 1,279 Food and Drug Administration (FDA)-approved compounds in this analysis, two compounds, sertraline (a serotonin reuptake inhibitor used as antidepressant) (73) and cefpiramide (a third-generation cephalosporin), generated metabolome profiles that were most similar to the metabolome of the arcA deletion strain (74) (Fig. 5A). Reciprocally, of \sim 3,800 gene deletions, arcA deletion was among the top 20 strains whose metabolomes were most similar to metabolome profiles generated by the two compounds. We reasoned that for the metabolome similarities to be physiologically meaningful and clinically relevant, the concentration of the drug needed to be equal to or less than the MIC for the Tet^R strain. While the sertraline concentration used in the metabolomics study was within MIC for Tet^R, the cefpiramide concentration in the metabolic profiling study (100 μ M, 61.3 μ g/ mL) (25) was higher than the estimated MIC ($<20~\mu g/mL$). Nonetheless, we performed a DiaMOND assay to evaluate a potential interaction between cefpiramide and tetracycline. An additive interaction was detected in the Tet^R strain (fractional inhibitory concentration $[FIC_2]$ score of \sim 1.2). Upon further exploration, we discovered that the metabolic pathways targeted by cefpiramide treatment were different from those affected upon the deletion of arcA (Fig. S6). Hence, this analysis demonstrated that while the metabolome similarity analysis helps to shortlist compounds, further analysis at the metabolic pathway level may be needed to ascertain whether the compounds might be synergistic due to a double hit on the same pathways (Fig. S6). We excluded cefpiramide from further analysis and proceeded to test whether sertraline could resensitize Tet^R E. coli to tetracycline.

Next, we also analyzed metabolomes of *E. coli* upon treatment with sertraline and deletion of arcA to discover that each perturbation individually resulted in the overactivation of TCA cycle, pyruvate metabolism, pentose phosphate pathway, butanoate metabolism, and inositol phosphate metabolism (Fig. S6). These findings suggested that treatment of the Tet^R $\Delta arcA$ strain with sertraline would likely lead to accumulation of toxic reactive oxygen species (ROS) due to overactivation of the TCA cycle (75). Consistent with the increased importance of ArcA-induced response in tetracycline resistance, sertraline (previously reported as bactericidal against *E. coli* [73]) was significantly more potent on the Tet^R strain (MIC: 35 μ g/mL), relative to the WT strain (MIC, 45 μ g/mL). Notably, deletion of arcA slightly increased the MIC of sertraline on WT (MIC, 50 μ g/mL). In contrast, sertraline was twice as potent upon knocking out arcA in the Tet^R background (MIC 17.5 μ g/mL; Fig. 5B). In other words, sertraline may kill *E. coli* by disrupting the ArcA network, and its increased activity on the Tet^R $\Delta arcA$ strain might amount to a double hit on the same network, providing a mechanistic explanation for why the two drugs are synergistic on Tet^R *E. coli* (73).

Finally, we performed a DiaMOND assay (76) to experimentally test the potential

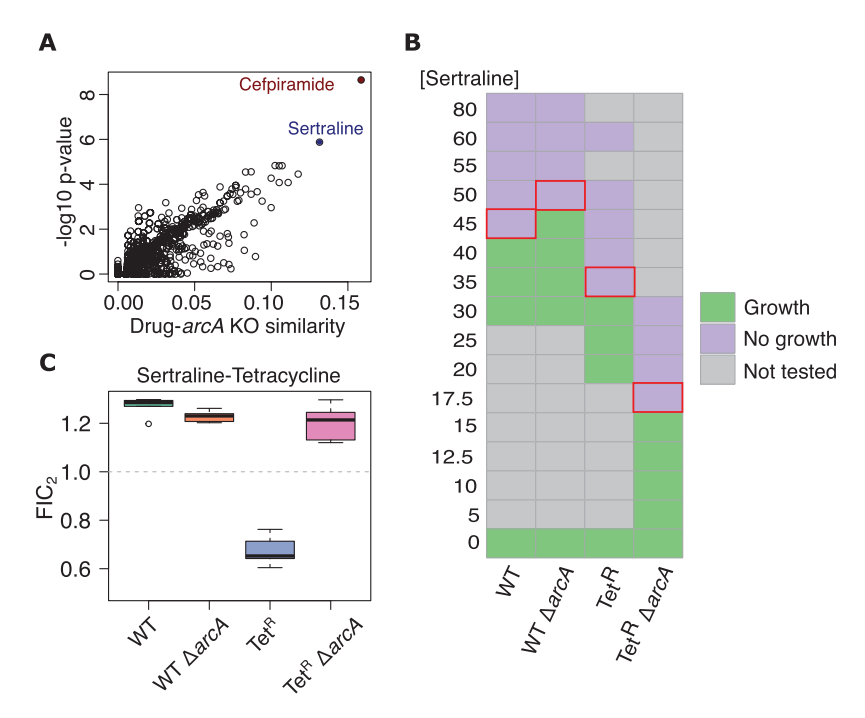


FIG 5 ArcA plays a central role in the synergistic effect of the sertraline-tetracycline combination in the tetracycline-resistant *E. coli.* (A) Analysis of similarity (estimated by pairwise comparison of *Z*-score-normalized profiles) between metabolic profiles of *E. coli* treated with 1,279 Food and Drug Administration (FDA)-approved compounds (25) and the metabolic profile of the *arcA E. coli* deletion strain (74), computed by Campos and Zampieri (25), identified sertraline and cefpiramide as promising candidate ArcA inhibitors. (B) Growth assays in a microdilution series (0 to 80 μ g/mL) were performed to assess dose response and susceptibility of different strains to sertraline (three biological replicates each one with three replicates for a total of nine replicates per strain/concentration). "Growth" indicates that for at least two replicates, the increase in OD₆₀₀ was higher than two times the maximum increase in OD₆₀₀ of control wells (inoculated with LB medium) after 16-h incubation. Red rectangles indicate the lowest concentration at which growth was not observed. (C) Results of DiaMOND assays to estimate fractional inhibitory concentration (FIC₂) for the sertraline-tetracycline combinations in the four strains (76). The data for five biological replicates per strain (six for Tet^R) are

mechanism of synergy between tetracycline and sertraline by investigating dose-dependent combinatorial effects of the two drugs on WT and Tet^R strains with and without *arcA* deletion (Fig. 5C). The activity of the tetracycline-sertraline combination was additive on the WT strain (FIC₂ score, \sim 1.27), with minimal change upon deletion of *arcA* (FIC₂ score, \sim 1.23). In stark contrast, the drug combination was potentially synergistic on the Tet^R strain (FIC₂ score, \sim 0.67), in agreement with previous reports of synergy between sertraline and tetracycline (73). Remarkably, the drug combination was additive on the Tet^R Δ arcA strain (FIC₂ score, 1.2), demonstrating unequivocally that the suggested synergy between tetracycline and sertraline emerges from disruption of the compensatory physiologic state that is mechanistically generated by increased ArcA activity.

DISCUSSION

We have discovered that global remodeling of transcription by a network of at least 25 TFs generates a novel metabolic state to compensate for loss of fitness that accompanies the gain of tetracycline resistance in *E. coli*. Interestingly, while the resistance mutations resulted in constitutive overexpression of the *acrAB* operon in the Tet^R strain, the global transcriptional remodeling manifested in a dramatic manner only during tetracycline treatment, suggesting that it was a downstream consequence of the increased activity of the AcrAB efflux pump. We propose a model to explain how increased efflux triggers a compensatory physiologic state to support tetracycline resistance in Tet^R *E. coli* (Fig. 6). AcrAB is an efflux pump of the RND superfamily that

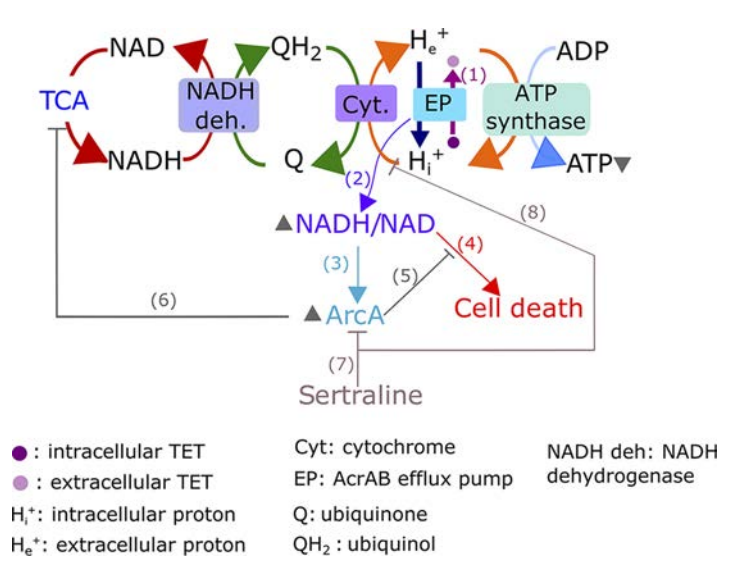


FIG 6 Summary overview of the ArcA-driven compensatory mechanism for tetracycline resistance and its connection with efflux pump mediated resistance. In the absence of tetracycline, Tet^R upregulates the *acrAB* efflux pump (EP), which in turn causes upregulation of fermentation-related genes (Fig. S1 and S2). The activity of AcrAB increases in the presence of tetracycline (30) (edge 1), driving dramatic changes in metabolism. We hypothesize that AcrAB disrupts the functions of other transporters by crowding the membrane, consuming the proton motive force (PMF), causing an increase in NADH/NAD ratio (edge 2) (Fig. 4E), which activates ArcA (71) (edge 3) (Fig. 2A). The potential toxic consequence of higher NADH/NAD ratio (49) (edge 4) is alleviated by ArcA (edge 5) through downregulation of the tricarboxylic acid (TCA) cycle (47) (edge 6). Finally, sertraline represses the ArcA network (edge 7) (Fig. 5A; Fig. S6) and putatively inhibits the PMF (73) (edge 8) to synergistically potentiate the bacteriostatic effect of tetracycline. Relative increases in abundance or activity are indicated with an upward pointing arrowhead, next to the corresponding molecule. Decreased concentration is indicated with a downward pointing arrowhead.

consumes the proton motive force (PMF) to expel intracellular substrates, tetracycline in this case (53). Hence, AcrAB competes with the ETC and ATP synthase both for space in the membrane and for the PMF, which is required for ATP synthesis (49). This competition may reduce oxidation of NADH molecules by the ETC, and the resulting increase in NADH/NAD ratio triggers ArcA. ArcA acts by repressing the TCA cycle and redirecting metabolic flux away from oxidative phosphorylation and toward overflow metabolism, which serves as an alternative source of energy (48, 50, 71, 72). This hypothesis is supported by two previously reported observations: (i) deleting either of the two repressors (marR and acrR) of the acrAB operon resulted in the increased secretion of acetate, a by-product of overflow metabolism (77); and (ii) mutations in acrB significantly reduced the rate of oxygen uptake (77). The downregulation of the TCA cycle may also serve to mitigate oxidative stress by preventing the production of ROS (75, 78). The global remodeling of the respiration and energy production pathways appears to be a generalized mechanism for restoring fitness across AMR pathogens, including P. aeruginosa (19) and Chromobacterium violaceum (24), that also manifest high intracellular NADH levels upon gaining resistance to diverse antibiotics through the increased expression of RND efflux pumps.

Amplification of the fitness cost of tetracycline resistance upon disrupting the master regulator (ArcA) of the compensatory metabolic state demonstrated how a network-based approach can rationally identify new vulnerabilities that emerge as a consequence of gaining resistance, because knocking out ArcA had a minor fitness consequence in the WT background (Fig. 3C and 4A). Having identified ArcA as a new vulnerability in the Tet^R strain, we were able to identify secondary molecule(s) that could target the compensatory physiologic state by leveraging the similarities between global metabolome changes in *E. coli* across a library of single-gene deletion strains and a drug library screen (25). By mining this publicly available metabolome comparison, we rank-prioritized the

most likely drugs in the screen that could disrupt the ArcA network to potentiate tetracycline action. Sertraline, which was among the top ranking candidates, was proposed to potentiate tetracycline action by blocking the PMF and indirectly inhibiting its efflux (73, 79, 80), albeit by a different plasmid-encoded TetA pump (27, 73). The loss of synergistic action of tetracycline-sertraline combination upon deleting arcA demonstrated the mechanism of synergy (Fig. 5C) but also revealed how Tet^R E. coli could (re)gain resistance and tolerance to this drug combination through a single regulatory mutation or transcriptional reprogramming of a single TF. Notably, the network analysis in this study implicated at least 25 TFs and their networks as mechanistic drivers of the compensatory physiologic state required to support the tetracycline resistance phenotype of Tet^R. This finding was supported by the dramatically different landscape of genome-wide fitness in the Tet^R strain background compared to the WT, which also illustrated how gaining resistance, at least by an efflux mechanism, is associated with system-wide trade-offs across multiple processes (Fig. 3). The complexity of this regulatory and metabolic network reprogramming also suggests that there are multiple routes through which a pathogen like E. coli could escape antibiotic treatment to gain resistance, explaining why we need multidrug combinations to combat antibiotic tolerance and resistance (81-83).

Formulating a multidrug regimen is particularly challenging because the numbers of combinations that need to be tested is too large, even for a high-throughput drug screen (84). A network-based approach, like the one described in this study and previously (81), will prove valuable in this effort because it uses a mechanistic model of a gene regulatory network underlying tolerance or resistance phenotypes to rankprioritize combinations of molecules that target multiple vulnerabilities within a pathogen. We have demonstrated that this strategy could enable the recovery of "lost" antibiotics by identifying new vulnerabilities that emerge within transcriptional and metabolic networks to manage trade-off in fitness upon gain of resistance (3, 19). This approach can be combined with laboratory evolution experiments to delineate trajectories of antibiotic resistance (85) and design drug combinations to preemptively curtail the emergence and spread of AMR. For instance, antibiotic-tolerant strains of E. coli gained resistance at a higher rate than the wild-type strain, suggesting that drugs that target the tolerance networks within these strains could potentially delay or block the emergence of resistance (85). Another high-throughput screen of a library of TF deletion strains demonstrated that deletion of arcA suppresses gain of resistance to cefixime, ciprofloxacin, and chloramphenicol (78). We posit that a multidrug regimen formulated based on vulnerabilities within networks governed by ArcA and other TFs identified in this study could have generalized value in extending the life spans of a broad range of existing antibiotics and supplement the development of new antimicrobial compounds (5).

MATERIALS AND METHODS

E. coli strains and culturing conditions. *E. coli* MG1655 (WT) and a lab-evolved tetracycline-resistant *E. coli* derived from the susceptible WT (Tet[®]) were kindly provided by Benno ter Kuile (32). *arcA* mutants were generated using the Red/ET recombination kit (Gene Bridges, Germany), following the manufacturer's instructions. Using this approach, a kanamycin cassette was inserted between the 5' and 3' regions of *arcA*. *arcA* disruption was confirmed with PCR and Sanger sequencing. *arcA* deletion was complemented with the pRB3-*arcA* plasmid (86) kindly provided by Sangwei Lu. *E. coli* strains were grown on Luria-Bertani (LB) broth on agar and broth (with constant shaking) at 37°C and aerobic conditions.

Assessment of arcA deletion effect on fitness. Microdilution growth curves were performed in LB broth using a Bioscreen C instrument (Growth Curves USA, Piscataway, NJ). First, frozen cells were used to streak individual colonies in LB plates (without antibiotic for WT and WT $\Delta arcA$, and with 4 μ g/mL of tetracycline [Sigma-Aldrich] for Tet^R, Tet^R $\Delta arcA$, and Tet^R $arcA^+$ [episomal complemented strain]). Isolated colonies were used to start tetracycline-free overnight cultures used as inoculum for the growth assays. Overnight cultures were adjusted to 0.01 Optical density at 600 nm (OD₆₀₀), and 200- μ L cultures with different concentrations of tetracycline (and other used compounds) were run at 37°C with continuous shaking. OD₆₀₀ was measured every 30 min. Wells inoculated only with LB were included to measure background OD₆₀₀ of the medium and as sterility controls. The Growthcurver R package (68) was used to fit a logistic equation to the OD₆₀₀ data for each well after subtracting its minimum OD₆₀₀ reading. Bacterial fitness was estimated in terms of the area under the growth curve (AUC) empirically determined by Growthcurver (68). The AUC value integrates multiple properties of the growth curve (69, 70).

For broth macrodilution experiments, four isolated colonies (from antibiotic-free LB plates for WT and WT $\Delta arcA$ and LB plates with 4 μ g/mL of tetracycline for Tet^R and Tet^R $\Delta arcA$) were used to start overnight LB cultures. Three overnight LB cultures per strain were diluted to 0.1 OD₆₀₀ in a final volume of 10 mL (in disposable culture tubes; Fisherbrand) with tetracycline (0.75 μ g/mL for WT and WT Δ arcA and 19.9 μ g/mL for Tet^R and Tet^R $\Delta arcA$) and without tetracycline (i.e., with addition of ethanol, used as solvent for tetracycline). As a control, the same volume of ethanol used for the tetracycline-treated samples was added to antibiotic-free cultures. These cultures were the starting point for the experiment. OD₆₀₀ was periodically measured using a SPECTRONIC 200E spectrophotometer (Thermo Scientific). To maintain cultures in mid-log phase, the cultures were diluted back to 0.1 OD₆₀₀ when they achieved an OD₆₀₀ of 1.0. Due to practical constraints, the cultures were considered in the target OD₆₀₀ range when they were in the 0.8 to 1.2 OD_{600} interval. Two sterile controls (containing only LB broth) were maintained throughout the experiments. All cultures were transferred after achieving the target OD₆₀₀ range for a total of three growth cycles (i.e., from 0.1 OD $_{600}$ to \sim 1.0 OD $_{600}$). The two controls were also transferred and followed for a total of three cycles until the end of the experiment. Sub-MIC tetracycline concentrations were selected based on moderate inhibition effects in Growthcurver-estimated maximum growth rates of microdilution growth curves (~60% for WT and between 53% and 76% for Tet^R treated with 0.75 and 20 μ g/mL of tetracycline, respectively), as performed previously by others (87).

Sertraline inhibitory concentration determination. We performed Bioscreen growth assays to assess the susceptibility of the different strains to sertraline (sertraline hydrochloride; Sigma-Aldrich). Growth assays covered a wide range of concentrations (for each compound/strain, we initially performed an exploratory experiment to define an optimal range including nine concentrations) for each compound of interest using three biological replicates (each one with three replicates for a total of nine replicates) per strain/concentration. Growth was defined as the instances in which two or more replicates increased their OD_{600} more than twice the maximum OD_{600} increment of the control wells (inoculated with sterile LB medium) after 16 h of incubation.

DiaMOND assay to evaluate synergy of two-drug combinations. We used the diagonal measurement of n-way drug interactions (DiaMOND) assay (76) (as described by Cokol-Cakmak et al. [88]) to evaluate the predicted ArcA-mediated synergy between tetracycline and selected compounds. Briefly, we first determined the single drug concentrations that reduced OD_{600} (measured after 16 h of growth) by half with respect to the drug-free condition (corresponding to the drug IC_{50}), using a BioTek Epoch 2 instrument (BioTek, USA). Spline fitting and the R Stats package were used to interpolate the IC_{50} values in the analyzed dose-response curves. Then, the IC_{50} values of the two-drug combinations (between tetracycline and selected compounds in a 1:1 volume using the IC_{50} concentrations defined in the previous step) were determined. The fractional inhibitory concentration for the two-drug combinations (FIC₂) under the Loewe additivity model was defined (76). Culture inoculums were prepared as described before. As the last step of the DiaMOND assay, five biological replicates (from independent colonies) were used to start five overnight cultures to measure the effect of the tetracycline-sertraline interaction. The raw data were visually inspected, and replicates with more than one potential IC_{50} or that grew better than expected (i.e., higher OD_{600}) in concentrations above the estimated IC_{50} were removed due to low confidence on the IC_{50} estimation.

NADH/NAD ratio measurements. NADH and NAD ratios were measured using the Enzychrom NAD/NADH assay kit (Bioassay Systems), following the manufacturer's instructions (and adding a sonication step of 20 s [89], before heating at 60°C for 5 min to lyse the bacterial cells). The equivalent of 1 mL of a 1.0 OD₆₀₀ bacterial culture was used to measure NAD and NADH concentrations. To simultaneously capture all bacterial cultures in log phase, overnight LB cultures (started from isolated colonies as previously explained for growth experiments) were adjusted to slightly different OD_{600} values to correct for differences in fitness among strains. Specifically, in the absence of tetracycline, the initial OD₆₀₀ values for WT, WT ΔarcA, Tet^R, and Tet^R ΔarcA were 0.015, 0.025, 0.04, and 0.07, respectively. In the presence of tetracycline (0.75 μ g/mL for WT and WT $\Delta arcA$ and 4 μ g/mL for Tet^R and Tet^R $\Delta arcA$), the initial OD₆₀₀ values were 0.02 (WT), 0.04 (WT $\Delta arcA$), and 0.05 (Tet^R and Tet^R $\Delta arcA$). A tetracycline concentration of 0.75 μ g/mL for WT and WT $\Delta arcA$ was selected based on its inhibitory effect (see above). For Tet^R and Tet^R Δ arcA, a tetracycline concentration of 4 μ g/mL was chosen based on the observation that fitness of both Tet^R and $\mathsf{Tet}^\mathsf{R}\Delta \mathit{arcA}$ was similar at the selected concentration (Fig. 4D). The selection was intended to minimize the impact of fitness differences (already detectable in the antibiotic-free condition; Fig. 4A) in the measured NADH/NAD ratio. NADH and NAD concentrations were measured after \sim 2.25 h (for cultures without tetracycline) and \sim 5.25 h (for cultures with tetracycline) of growth at 37°C. Final results included three to six replicates per strain.

Differential expression analysis of *E. coli* MG1655 and tetracycline-resistant MG1655 microarray data. To characterize the adaptation of the Tet^R strain to tetracycline, we analyzed publicly available normalized microarray data for the WT and Tet^R strains in the presence and absence of tetracycline (Gene Expression Omnibus accession number GSE57084) reported by Händel et al. (32). Differential expression analysis of microarray data was performed using a Bayesian t test with the Cyber-T tool (90). Genes with adjusted P values < 0.05 and absolute \log_2 fold change >1 were considered differentially expressed. Transcriptional profiles of arcA deletion strains (GEO accession numbers GSE1121 and GSE46415) (46, 47) were analyzed using the same thresholds.

Functional enrichment analysis. Enrichment analyses of significantly up- and downregulated set of genes were independently performed using DAVID (91). Only functional terms with adjusted P values (Benjamini-Hochberg) < 0.05 were considered enriched. When using DAVID functional term clustering results, general themes were manually defined for significant term clusters (i.e., with scores > 1.3 as recommended by DAVID developers).

Identification of differentially active regulatory circuits associated with the gain of tetracycline

resistance. We identified differentially active TFs using the NetSurgeon algorithm (41), as previously applied for Mycobacterium tuberculosis (92). Briefly, NetSurgeon ranks TFs based on their potential influence in the observed transcriptional changes between two states of interest (estimated according to the change in expression of their known target genes) (41). A total of 192 TF regulons were extracted from a transcriptional network (containing 5,517 signed TF-gene interactions) compiled from the RegulonDB version 9.0 database (40). Of the 192 TFs, 68 had less than 5 target genes and were not included in the analysis to reduce false positives due to overlap between regulons. We focused on the transcriptional changes between the Tet^R strain and the parental WT strain in the absence of tetracycline and the response of the Tet^R strain to tetracycline. TFs ranked (using the highest score between the independently computed scores for increased activity and decreased activity) in the top 15 of each comparison were considered differentially active. To complement the NetSurgeon analysis, a network component analysis (43) was applied to estimate the TF activity (TFA) using the transcriptional profile of their known targets. The RegulonDB-derived transcriptional network mentioned above and the microarray data reported by Händel et al. were used to estimate the TFA as previously described (32, 93). Statistical differences in TF activity were determined using a Welch's t test. Only TFs with adjusted P values of < 0.05for basal and adaptive response that agreed with NetSurgeon-based predictions (Table 1) were considered differentially active. Finally, we mined the EGRIN model previously developed for E. coli (44) to identify clusters of coregulated genes statistically enriched (with adjusted hypergeometric test P values ≤ 0.05 and containing >9 DEGs) with genes whose expression was altered by gain of tetracycline resistance. The association between clusters with differentially expressed genes and TF regulons was used as an indicator of differential activity of the relevant TFs.

Characterization of metabolic response of *E. coli* to drug treatment and *arcA* deletion. We used the MetaboAnalyst 5.0 website (94) to analyze publicly available *Z*-score-normalized metabolic profiles of sertraline- and cefpiramide-treated *E. coli* (25) and *arcA* deletion *E. coli* (74). For each condition, the affected metabolites were defined as the ones within the highest 10% of absolute *Z* scores. To identify metabolically altered pathways due to drug treatments, we used the "pathway analysis" module available in the MetaboAnalyst platform using the hypergeometric test, relative-betweenness centrality, and the *E. coli* KEGG pathway library options. The input for this analysis was the KEGG IDs associated with perturbed metabolites. Only metabolic pathways with false discovery rate-adjusted hypergeometric test *P* values ≤ 0.25 were considered altered, following the threshold suggested by MetaboAnalyst developers. Similarly, we used the "joint-pathway analysis" module to identify metabolic pathways affected by he *arcA* deletion. This analysis integrated a list of DEGs due to *arcA* deletion (47) and a list of metabolites responding to *arcA* deletion (defined as described above) using the "metabolic pathways (integrated)," "hypergeometric test," "relative-betweenness centrality," and "combine queries" options for *E. coli*. Altered pathways were defined with the same adjusted *P* value threshold described above.

Genome sequencing. Late-log phase WT broth cultures were spun down, and the cells were lysed with lysis buffer (0.1% SDS, 0.1 M dithiothreitol [DTT], 10 mg/mL lysozyme in 0.1 M Tris-EDTA [TE] buffer). DNA was isolated from cell lysate using phenol-chloroform-isoamyl alcohol extraction method. Overnight Tet^R broth cultures were spun down. Cell pellets were resuspended in TE buffer. 10% SDS and proteinase K were added. DNA was precipitated with 100% ethanol added in a 3:1 volume ratio. The genomic DNA precipitate was washed with 70% ethanol and later dried out. Libraries for sequencing were prepared with the Nextera XT DNA library preparation kit (Illumina, San Diego, CA) for paired-end sequencing in a NextSeq instrument.

Identification of mutations in the Tet^R **strain.** Initial quality check and trimming of raw FASTQ files was performed using Trimmomatic 0.39 (95), with the following parameters: ILLUMINACLIP:NexteraPE-PE.fa:2:30:10, LEADING:3, TRAILING:3, SLIDINGWINDOW:4:15, and MINLEN:36. Reads that survived this filtering step were used for identifying mutations in the Tet^R strain, while taking into account background mutations present in the parental WT strain. Variant calling was performed with Snippy version 4.6.0 (https://github.com/tseemann/snippy) using default parameters and *E. coli* K-12 MG1655 genome (NC_000913.3) as a reference. Genomic coverage and identified variants are listed in Table S1.

Genome-wide CRISPR KO library construction on Onyx. Genome-wide KO libraries in WT and Tet^R background *E. coli* strains were generated on the Onyx Digital Genome Engineering Platform, a commercial benchtop instrument sold by Inscripta, Inc. Onyx (catalog number 1001176) is an automated platform that uses the MAD7 nuclease, a type V CRISPR nuclease from *Eubacterium rectale*, to generate multiplexed genome engineered libraries. All consumables, assays, and software used in this study are available at https://portal.inscriptacp.com/.

Compatibility of genome-wide libraries designed for WT *E. coli* with the Tet^R strain was confirmed by *de novo* genome assembly using short read polishing of Nanopore-based long reads using Raven (96) and Racon (97). Inscripta's Onyx microbial strain analyzer (OMSA) tool was used to confirm that 99.9% of designs in the library are predicted to function in the Tet^R strain background. The genome-wide KO library included 8,271 intended edits representing approximately two deletion mutants per gene: a triple-stop (TAATAATAA) substitution at amino acid position 10 and a triple-stop insertion at amino acid position 15.

Single *E. coli* WT or Tet^R colonies were isolated from an LB agar plate and grown overnight in LB to saturation and diluted to optical density at 600 nm (OD_{600}) of 2.5 before subsequent processing. 1 mL of cell suspension was subsequently prepared using the Onyx *E. coli* edit competency kit (GEN-EC-1004). 1 mL of *E. coli* cells (approximately 6 × 10⁸ cells) prepared using the edit competency kit were placed into the Onyx instrument. The OnyxWare program K-strain version 1.1 was selected, and the Onyx run was initiated. Briefly, the instrument transferred the cells to a cell growth cuvette (reference number 1001155/catalog number GEN-EC-1007) for growth to 0.5 OD₆₀₀, as measured on the instrument. After

an initial outgrowth, the instrument transferred cells to the microfluidic cell controller (reference number 1001152/catalog number GEN-EC-1007). There, the cells were prepared for electroporation using media exchange. Once they were rendered competent, the instrument moved the cells to the microfluidic cell transformer (reference number 1001152/catalog number GEN-EC-1007), which controls introduction of the MAD7-containing "engine" plasmid, as well as the gRNA/repair template/barcode-containing plasmid into cells by electroporation. Following electroporation, the cells were placed by the instrument into a second cell growth cuvette (reference number 1002161/catalog number GEN-EC-1007) for recovery. The cells were then transferred to the digital engineering processor (reference number 1001153/catalog number GEN-EC-1007) for abundance normalization. The resulting normalized pool of cells was collected as multiple tubes from the instrument. Per library, 5 mL of cells were collected at an OD₆₀₀ ranging from 3.2 to 3.7. The cells were immediately stored frozen at -80° C in 15.5% glycerol. Depending on cell growth, the total run time on the instrument for *E. coli* lasted around 48 h.

Following editing, the pooled libraries were grown off-instrument for approximately 8 h in TB supplemented with 1,000 μ g/mL carbenicillin and 68 μ g/mL chloramphenicol. Library edit fractions were estimated using pooled whole-genome sequencing (pWGS) and ranged from 45.3 to 50.8% (98). Based on statistical approaches described by Cawley et al. (98), we expect to observe 96.9 to 97.1% of all designs in selections using these libraries, assuming the selections start with $\geq 1 \times 10^6$ cells.

Competitive assays of pooled mutant libraries. To evaluate the impact of single-gene deletions in the fitness of the Tet^R strain, we performed broth macrodilution growth experiments as described before. Notably, instead of using overnight cultures as inocula, we grew five aliquots (each with 0.2 mL, previously stored at -80° C) of the relevant library in LB with 99.9 μ g/mL of carbenicillin for 4 to 6 h (we refer to these cultures as the library acclimatization cultures, or "t0"). Carbenicillin was added along all experiments to maintain the plasmid harboring DNA barcodes for each gene edit. For each library, four acclimatization cultures were used to start four 0.1 OD₆₀₀ 10-mL LB cultures with tetracycline (0.75 μ g/mL for WT libraries and 20 μ g/mL for Tet^R libraries) and without tetracycline (i.e., adding ethanol as a control as previously explained). Sub-MIC tetracycline concentrations were selected as explained before. Pooled library cultures were maintained in mid-log phase during three growth cycles (i.e., from 0.1 OD₆₀₀ to \sim 1.0 OD₆₀₀). At the end of each growth cycle (i.e., when cultures were in the 0.8 to 1.2 OD₆₀₀ interval), culture aliquots were used to create cell pellets stored at -80° C. Cell pellets of the acclimatization cultures were also stored. As in previous experiments, two control LB cultures were included in each experiment.

Barcode sequencing fitness estimation. Cell pellets from the competition assays described in the previous section were used for DNA extraction following Inscripta protocol with the Wizard SV genomic DNA purification system (Promega). DNA libraries of previously extracted DNA were prepared using the 48-sample Onyx barcode diversity assay kit (Inscripta, Boulder, CO) following the manufacturer's instructions. Four available replicates of each analyzed mutant library were sequenced. Prepared libraries were sequenced (as single-end 100-bp reads) in a NextSeq instrument. An average of 972 (± 321) reads per design for each replicate was observed.

Raw sequencing data were processed on Illumina BaseSpace suite. The resulting FASTQ files were processed with the InscriptaResolver software to estimate read counts for each gene deletion (Data Set S1). We used the number of reads for each unique gene edit barcode sequence as a proxy for mutant frequency in the genome-wide single-gene deletion competition assays in order to identify mutants over- and under-represented in the population. In this way, we were able to identify mutations that were deleterious (under-represented) or beneficial (over-represented). The ALDEx2 R package (51) was used to identify differentially abundant gene deletion designs. Briefly, we used ALDEx2 interquartile log ratio transformation to estimate relative abundance of each mutant with 1,000 Monte Carlo instances. Before each comparison, we removed all deletion mutants with less than 10 reads in all four replicates (referred to as 'dropouts') of any of the two time points being compared. We define differentially abundant mutants at 't1' and 't2' with respect to 't0' as those constructs with Benjamini-Hochberg adjusted (Welch's and Wilcoxon) t test P values < 0.1 and absolute ALDEx2-estimated effect >2, as suggested by ALDEx2 developers and others (99, 100). Changes in abundance for each KO design at each time point (with respect to t0) correspond to ALDEx2-computed "diff.btw" scores. Data for the last time point (t3) was not used in this analysis due to the high number of depleted mutants at the end of the experiment (due to tetracycline selection pressure) (Fig. 3A) and the challenge this may represent for ALDEx2 posterior relative abundance estimation (51). To focus on the genes most likely affecting fitness, a gene was only considered to affect fitness if all of its deletion mutants (excluding any dropout) were differentially abundant and had the same effect (deleterious or beneficial).

Code availability. An R notebook (101) with all necessary scripts and input files to generate all figures of this article are publicly available in the following GitHub repository: https://github.com/marioluisao/Compensatory-mechanisms-for-Antimicrobial-Resistance.

Materials availability. Material requests may be directed to the corresponding author, Nitin S. Baliqa (nitin.baliqa@isbscience.org).

Data availability. The data generated in this study are available in the following GitHub repository: https://github.com/marioluisao/Compensatory-mechanisms-for-Antimicrobial-Resistance.

SUPPLEMENTAL MATERIAL

Supplemental material is available online only.

DATA SET S1, XLSX file, 12.1 MB.

DATA SET S2, XLSX file, 0.1 MB.

FIG S1, PDF file, 0.04 MB.

FIG S2, PDF file, 0.03 MB.

FIG S3, PDF file, 0.2 MB.

FIG S4, PDF file, 0.1 MB.

FIG S5, PDF file, 0.03 MB.

FIG S6, PDF file, 0.2 MB.

TABLE S1, DOCX file, 0.02 MB.

TABLE S2, DOCX file, 0.02 MB.

ACKNOWLEDGMENTS

We thank members of the Baliga lab for critical discussions and feedback. We especially thank Jacob Valenzuela for his feedback on the competition assay experimental design. We thank Benno ter Kuile at University of Amsterdam for kindly providing the *E. coli* strains used in this study. We also thank Sangwei Lu at University of California Berkeley for kindly providing the pRB3-*arcA* plasmid. Finally, we also thank the Molecular and Cell Core Facility of the Institute for Systems Biology.

This work was supported by National Science Foundation grants DBI-1565166 and IIBR-2042948 and National Institutes of Health grants R01AI141953 and R01AI128215 (N.S.B.).

A.N.B. and T.R.S. are affiliated with Inscripta, Inc. Inscripta, Inc., contributed reagents for this study.

N.S.B. and M.L.A.-O. conceptualized the study and designed the research. M.L.A.-O., M.P., E.P.-T., A.K., V.S., and A.D. performed experiments. M.L.A.-O., V.S., S.R.C.I. performed computational analyses. T.R.S. and A.N.B. designed and constructed the CRISPR-Cas deletion libraries, and estimated gene count per mutant. M.L.A.-O. and N.S.B. analyzed data and wrote the manuscript. N.S.B. provided supervision.

REFERENCES

- Blair JMA, Webber MA, Baylay AJ, Ogbolu DO, Piddock LV. 2015. Molecular mechanisms of antibiotic resistance. Nat Rev Microbiol 13:42–51. https://doi.org/10.1038/nrmicro3380.
- Brauner A, Fridman O, Gefen O, Balaban NQ. 2016. Distinguishing between resistance, tolerance and persistence to antibiotic treatment. Nat Rev Microbiol 14:320–330. https://doi.org/10.1038/nrmicro.2016.34.
- Andersson DI, Hughes D. 2010. Antibiotic resistance and its cost: is it possible to reverse resistance? Nat Rev Microbiol 8:260–271. https://doi.org/10.1038/nrmicro2319.
- O'Neill J. 2016. Tackling drug-resistant infections globally: final report and recommendations. *In Review on Antimicrobial Resistance*. Wellcome Trust and HM Government. https://amr-review.org/sites/default/files/ 160525_Final%20paper_with%20cover.pdf.
- 5. Ventola CL. 2015. The antibiotic resistance crisis: part 1: causes and threats. Pharm Ther 40:277.
- Zhang Q-Q, Ying G-G, Pan C-G, Liu Y-S, Zhao J-L. 2015. Comprehensive evaluation of antibiotics emission and fate in the river basins of China: source analysis, multimedia modeling, and linkage to bacterial resistance. Environ Sci Technol 49:6772–6782. https://doi.org/10.1021/acs.est 5b00729
- Kohanski MA, DePristo MA, Collins JJ. 2010. Sublethal antibiotic treatment leads to multidrug resistance via radical-induced mutagenesis. Mol Cell 37:311–320. https://doi.org/10.1016/j.molcel.2010.01.003.
- Long H, Miller SF, Strauss C, Zhao C, Cheng L, Ye Z, Griffin K, Te R, Lee H, Chen C-C, Lynch M. 2016. Antibiotic treatment enhances the genomewide mutation rate of target cells. Proc Natl Acad Sci U S A 113: E2498–E2505.
- Kollef MH, Fraser VJ. 2001. Antibiotic resistance in the intensive care unit. Ann Intern Med 134:298–314. https://doi.org/10.7326/0003-4819-134-4-200102200-00014.
- Murray CJL, Ikuta KS, Sharara F, Swetschinski L, Aguilar GR, Gray A, Han C, Bisignano C, Rao P, Wool E, Antimicrobial Resistance Collaborators. 2022. Global burden of bacterial antimicrobial resistance in 2019: a systematic analysis. Lancet 399:629–655. https://doi.org/10.1016/S0140-6736(21)02724-0.

- Mölstad S, Erntell M, Hanberger H, Melander E, Norman C, Skoog G, Lundborg CS, Söderström A, Torell E, Cars O. 2008. Sustained reduction of antibiotic use and low bacterial resistance: 10-year follow-up of the Swedish Strama programme. Lancet Infect Dis 8:125–132. https://doi .org/10.1016/S1473-3099(08)70017-3.
- 12. Weis SE, Slocum PC, Blais FX, King B, Nunn M, Matney GB, Gomez E, Foresman BH. 1994. The effect of directly observed therapy on the rates of drug resistance and relapse in tuberculosis. N Engl J Med 330: 1179–1184. https://doi.org/10.1056/NEJM199404283301702.
- Cars O, Mölstad S, Melander A. 2001. Variation in antibiotic use in the European Union. Lancet 357:1851–1853. https://doi.org/10.1016/S0140-6736(00)04972-2.
- Fernandes P, Martens E. 2017. Antibiotics in late clinical development. Biochem Pharmacol 133:152–163. https://doi.org/10.1016/j.bcp.2016.09 .025.
- 15. Lewis K. 2013. Platforms for antibiotic discovery. Nat Rev Drug Discov 12: 371–387. https://doi.org/10.1038/nrd3975.
- Suzuki S, Horinouchi T, Furusawa C. 2014. Prediction of antibiotic resistance by gene expression profiles. Nat Commun 5:5792. https://doi.org/ 10.1038/ncomms6792.
- Dunphy LJ, Yen P, Papin JA. 2019. Integrated experimental and computational analyses reveal differential metabolic functionality in antibiotic-resistant *Pseudomonas aeruginosa*. Cell Syst 8:3–14.e3. https://doi.org/10.1016/j.cels.2018.12.002.
- Webber MA, Ricci V, Whitehead R, Patel M, Fookes M, Ivens A, Piddock LV. 2013. Clinically relevant mutant DNA gyrase alters supercoiling, changes the transcriptome, and confers multidrug resistance. mBio 4: e00273-13. https://doi.org/10.1128/mBio.00273-13.
- Pacheco JO, Alvarez-Ortega C, Rico MA, Martinez JL. 2017. Metabolic compensation of fitness costs is a general outcome for antibiotic-resistant *Pseudomonas aeruginosa* mutants overexpressing efflux pumps. mBio 8:e00500-17. https://doi.org/10.1128/mBio.00500-17.
- 20. Freihofer P, Akbergenov R, Teo Y, Juskeviciene R, Andersson DI, Böttger EC. 2016. Nonmutational compensation of the fitness cost of antibiotic

- resistance in mycobacteria by overexpression of tlyA rRNA methylase. RNA 22:1836–1843. https://doi.org/10.1261/rna.057257.116.
- Ejim L, Farha MA, Falconer SB, Wildenhain J, Coombes BK, Tyers M, Brown ED, Wright GD. 2011. Combinations of antibiotics and nonantibiotic drugs enhance antimicrobial efficacy. Nat Chem Biol 7:348–350. https://doi.org/10.1038/nchembio.559.
- Baym M, Stone LK, Kishony R. 2016. Multidrug evolutionary strategies to reverse antibiotic resistance. Science 351:aad3292. https://doi.org/10 .1126/science.aad3292.
- Peng BO, Su Y, Li H, Han YI, Guo C, Tian Y, Peng X. 2015. Exogenous alanine and/or glucose plus kanamycin kills antibiotic-resistant bacteria. Cell Metab 21:249–262. https://doi.org/10.1016/j.cmet.2015.01.008.
- Banerjee D, Parmar D, Bhattacharya N, Ghanate AD, Panchagnula V, Raghunathan A. 2017. A scalable metabolite supplementation strategy against antibiotic resistant pathogen *Chromobacterium violaceum* induced by NAD⁺/NADH⁺ imbalance. BMC Syst Biol 11:1–20. https://doi.org/10.1186/s12918-017-0427-z.
- Campos Al, Zampieri M. 2019. Metabolomics-driven exploration of the chemical drug space to predict combination antimicrobial therapies. Mol Cell 74:1291–1303.e6. https://doi.org/10.1016/j.molcel.2019.04.001.
- Roberts MC. 1996. Tetracycline resistance determinants: mechanisms of action, regulation of expression, genetic mobility, and distribution. FEMS Microbiol Rev 19:1–24. https://doi.org/10.1111/j.1574-6976.1996.tb00251.x.
- Thaker M, Spanogiannopoulos P, Wright GD. 2010. The tetracycline resistome. Cell Mol Life Sci 67:419–431. https://doi.org/10.1007/s00018-009-0172-6.
- Center for Veterinary Medicine. 2018. Summary report on antimicrobials sold or distributed for use in food-producing animals. U.S. Food and Drug Administration, Silver Spring, MD.
- Nelson ML, Levy SB. 1999. Reversal of tetracycline resistance mediated by different bacterial tetracycline resistance determinants by an inhibitor of the Tet (B) antiport protein. Antimicrob Agents Chemother 43: 1719–1724. https://doi.org/10.1128/AAC.43.7.1719.
- Viveiros M, Jesus A, Brito M, Leandro C, Martins M, Ordway D, Molnar AM, Molnar J, Amaral L. 2005. Inducement and reversal of tetracycline resistance in *Escherichia coli* K-12 and expression of proton gradient-dependent multidrug efflux pump genes. Antimicrob Agents Chemother 49:3578–3582. https://doi.org/10.1128/AAC.49.8.3578-3582.2005.
- van der Horst MA, Schuurmans JM, Smid MC, Koenders BB, ter Kuile BH.
 2011. De novo acquisition of resistance to three antibiotics by Escherichia coli. Microb Drug Resist 17:141–147. https://doi.org/10.1089/mdr.2010.0101.
- Händel N, Schuurmans JM, Feng Y, Brul S, ter Kuile BH. 2014. Interaction between mutations and regulation of gene expression during development of de novo antibiotic resistance. Antimicrob Agents Chemother 58: 4371–4379. https://doi.org/10.1128/AAC.02892-14.
- Hoeksema M, Jonker MJ, Brul S, ter Kuile BH. 2019. Effects of a previously selected antibiotic resistance on mutations acquired during development of a second resistance in *Escherichia coli*. BMC Genomics 20:284. https://doi.org/10.1186/s12864-019-5648-7.
- Malinverni JC, Silhavy TJ. 2009. An ABC transport system that maintains lipid asymmetry in the Gram-negative outer membrane. Proc Natl Acad Sci U S A 106:8009–8014. https://doi.org/10.1073/pnas.0903229106.
- Pankey GA. 2005. Tigecycline. J Antimicrob Chemother 56:470–480. https://doi.org/10.1093/jac/dki248.
- He F, Xu J, Wang J, Chen Q, Hua X, Fu Y, Yu Y. 2016. Decreased susceptibility to tigecycline mediated by a mutation in mlaA in *Escherichia coli* strains. Antimicrob Agents Chemother 60:7530–7531. https://doi.org/10.1128/AAC.01603-16.
- 37. Hobbs EC, Yin X, Paul BJ, Astarita JL, Storz G. 2012. Conserved small protein associates with the multidrug efflux pump AcrB and differentially affects antibiotic resistance. Proc Natl Acad Sci U S A 109:16696–16701. https://doi.org/10.1073/pnas.1210093109.
- de Cristobal RE, Vincent PA, Salomon RA. 2006. Multidrug resistance pump AcrAB-TolC is required for high-level, Tet(A)-mediated tetracycline resistance in *Escherichia coli*. J Antimicrob Chemother 58:31–36. https:// doi.org/10.1093/jac/dkl172.
- 39. Nichols RJ, Sen S, Choo YJ, Beltrao P, Zietek M, Chaba R, Lee S, Kazmierczak KM, Lee KJ, Wong A, Shales M, Lovett S, Winkler ME, Krogan NJ, Typas A, Gross CA. 2011. Phenotypic landscape of a bacterial cell. Cell 144:143–156. https://doi.org/10.1016/j.cell.2010.11.052.
- Gama-Castro S, Salgado H, Santos-Zavaleta A, Ledezma-Tejeida D, Muñiz-Rascado L, García-Sotelo JS, Alquicira-Hernández K, Martínez-Flores I, Pannier L, Castro-Mondragón JA, Medina-Rivera A, Solano-Lira

- H, Bonavides-Martínez C, Pérez-Rueda E, Alquicira-Hernández S, Porrón-Sotelo L, López-Fuentes A, Hernández-Koutoucheva A, Del Moral-Chávez V, Rinaldi F, Collado-Vides J. 2016. RegulonDB version 9.0: high-level integration of gene regulation, coexpression, motif clustering and beyond. Nucleic Acids Res 44:D133–D134. https://doi.org/10.1093/nar/gkv1156.
- Michael DG, Maier EJ, Brown H, Gish SR, Fiore C, Brown RH, Brent MR. 2016. Model-based transcriptome engineering promotes a fermentative transcriptional state in yeast. Proc Natl Acad Sci U S A 113:E7428–E7437.
- Duval V, Lister IM. 2013. MarA, SoxS and Rob of *Escherichia coli*—Global regulators of multidrug resistance, virulence and stress response. Int J Biotechnol Wellness Ind 2:101–124. https://doi.org/10.6000/1927-3037 2013.02.03.2
- 43. Liao JC, Boscolo R, Yang Y-L, Tran LM, Sabatti C, Roychowdhury VP. 2003. Network component analysis: reconstruction of regulatory signals in biological systems. Proc Natl Acad Sci U S A 100:15522–15527. https://doi.org/10.1073/pnas.2136632100.
- 44. Brooks AN, Reiss DJ, Allard A, Wu W-J, Salvanha DM, Plaisier CL, Chandrasekaran S, Pan M, Kaur A, Baliga NS. 2014. A system-level model for the microbial regulatory genome. Mol Syst Biol 10:740. https://doi.org/10.15252/msb.20145160.
- 45. Shalel-Levanon S, San K-Y, Bennett GN. 2005. Effect of oxygen, and ArcA and FNR regulators on the expression of genes related to the electron transfer chain and the TCA cycle in *Escherichia coli*. Metab Eng 7: 364–374. https://doi.org/10.1016/j.ymben.2005.07.001.
- 46. Covert MW, Knight EM, Reed JL, Herrgard MJ, Palsson BO. 2004. Integrating high-throughput and computational data elucidates bacterial networks. Nature 429:92–96. https://doi.org/10.1038/nature02456.
- 47. Park DM, Akhtar MS, Ansari AZ, Landick R, Kiley PJ. 2013. The bacterial response regulator ArcA uses a diverse binding site architecture to regulate carbon oxidation globally. PLoS Genet 9:e1003839. https://doi.org/10.1371/journal.pgen.1003839.
- 48. Basan M, Hui S, Williamson JR. 2017. ArcA overexpression induces fermentation and results in enhanced growth rates of *E. coli*. Sci Rep 7:1–7. https://doi.org/10.1038/s41598-017-12144-6.
- Szenk M, Dill KA, de Graff AMR. 2017. Why do fast-growing bacteria enter overflow metabolism? Testing the membrane real estate hypothesis. Cell Syst 5:95–104. https://doi.org/10.1016/j.cels.2017.06.005.
- Basan M, Hui S, Okano H, Zhang Z, Shen Y, Williamson JR, Hwa T. 2015. Overflow metabolism in *Escherichia coli* results from efficient proteome allocation. Nature 528:99–104. https://doi.org/10.1038/ nature15765.
- 51. Fernandes AD, Reid JN, Macklaim JM, McMurrough TA, Edgell DR, Gloor GB. 2014. Unifying the analysis of high-throughput sequencing datasets: characterizing RNA-seq, 16S rRNA gene sequencing and selective growth experiments by compositional data analysis. Microbiome 2:15–13. https://doi.org/10.1186/2049-2618-2-15.
- 52. Mika F, Hengge R. 2005. A two-component phosphotransfer network involving ArcB, ArcA, and RssB coordinates synthesis and proteolysis of $\sigma^{\rm S}$ (RpoS) in *E. coli*. Genes Dev 19:2770–2781. https://doi.org/10.1101/gad.353705.
- Anes J, McCusker MP, Fanning S, Martins M. 2015. The ins and outs of RND efflux pumps in *Escherichia coli*. Front Microbiol 6:587. https://doi.org/10.3389/fmicb.2015.00587.
- 54. Thiagalingam S, Grossman L. 1991. Both ATPase sites of *Escherichia coli* UvrA have functional roles in nucleotide excision repair. J Biol Chem 266: 11395–11403. https://doi.org/10.1016/S0021-9258(18)99176-3.
- Ragheb MN, Thomason MK, Hsu C, Nugent P, Gage J, Samadpour AN, Kariisa A, Merrikh CN, Miller SI, Sherman DR, Merrikh H. 2019. Inhibiting the evolution of antibiotic resistance. Mol Cell 73:157–165.e5. https://doi .org/10.1016/j.molcel.2018.10.015.
- Jones HM, Gunsalus RP. 1987. Regulation of *Escherichia coli* fumarate reductase (frdABCD) operon expression by respiratory electron acceptors and the fnr gene product. J Bacteriol 169:3340–3349. https://doi.org/10.1128/jb.169.7.3340-3349.1987.
- 57. Suvarna K, Stevenson D, Meganathan R, Hudspeth MES. 1998. Menaquinone (vitamin K₂) biosynthesis: localization and characterization of the menA gene from *Escherichia coli*. J Bacteriol 180:2782–2787. https://doi.org/10.1128/JB.180.10.2782-2787.1998.
- Hiratsuka T, Furihata K, Ishikawa J, Yamashita H, Itoh N, Seto H, Dairi T. 2008.
 An alternative menaquinone biosynthetic pathway operating in microorganisms. Science 321:1670–1673. https://doi.org/10.1126/science.1160446.
- 59. Cole ST, Eiglmeier K, Ahmed S, Honore N, Elmes L, Anderson WF, Weiner JH. 1988. Nucleotide sequence and gene-polypeptide relationships of

- the glpABC operon encoding the anaerobic *sn*-glycerol-3-phosphate dehydrogenase of *Escherichia coli* K-12. J Bacteriol 170:2448–2456. https://doi.org/10.1128/jb.170.6.2448-2456.1988.
- Lubitz SP, Weiner JH. 2003. The Escherichia coli ynfEFGHI operon encodes polypeptides which are paralogues of dimethyl sulfoxide reductase (DmsABC). Arch Biochem Biophys 418:205–216. https://doi.org/10.1016/j.abb.2003.08.008.
- Jormakka M, Tornroth S, Byrne B, Iwata S. 2002. Molecular basis of proton motive force generation: structure of formate dehydrogenase-N. Science 295:1863–1868. https://doi.org/10.1126/science.1068186.
- Menon NK, Chatelus CY, Dervartanian M, Wendt JC, Shanmugam KT, Peck HD, Jr, Przybyla AE. 1994. Cloning, sequencing, and mutational analysis of the hyb operon encoding *Escherichia coli* hydrogenase 2. J Bacteriol 176: 4416–4423. https://doi.org/10.1128/jb.176.14.4416-4423.1994.
- Park S-J, Cotter PA, Gunsalus RP. 1995. Regulation of malate dehydrogenase (mdh) gene expression in Escherichia coli in response to oxygen, carbon, and heme availability. J Bacteriol 177:6652–6656. https://doi .org/10.1128/jb.177.22.6652-6656.1995.
- Zwir I, Shin D, Kato A, Nishino K, Latifi T, Solomon F, Hare JM, Huang H, Groisman EA. 2005. Dissecting the PhoP regulatory network of *Escherichia coli* and *Salmonella* enterica. Proc Natl Acad Sci U S A 102: 2862–2867. https://doi.org/10.1073/pnas.0408238102.
- 65. Battesti A, Majdalani N, Gottesman S. 2011. The RpoS-mediated general stress response in *Escherichia coli*. Annu Rev Microbiol 65:189–213. https://doi.org/10.1146/annurev-micro-090110-102946.
- Gerlach P, Valentin-Hansen P, Bremer E. 1990. Transcriptional regulation of the cytR repressor gene of *Escherichia coli*: autoregulation and positive control by the cAMP/CAP complex. Mol Microbiol 4:479–488. https://doi .org/10.1111/j.1365-2958.1990.tb00614.x.
- Lauritsen I, Frendorf PO, Capucci S, Heyde SAH, Blomquist SD, Wendel S, Fischer EC, Sekowska A, Danchin A, Nørholm MHH. 2021. Temporal evolution of master regulator Crp identifies pyrimidines as catabolite modulator factors. Nat Commun 12:1–13. https://doi.org/10.1038/s41467-021-26098-x.
- Sprouffske K, Wagner A. 2016. Growthcurver: an R package for obtaining interpretable metrics from microbial growth curves. BMC Bioinformatics 17:172. https://doi.org/10.1186/s12859-016-1016-7.
- Palmer AC, Toprak E, Baym M, Kim S, Veres A, Bershtein S, Kishony R. 2015. Delayed commitment to evolutionary fate in antibiotic resistance fitness landscapes. Nat Commun 6:1–8. https://doi.org/10.1038/ncomms8385.
- Dunai A, Spohn R, Farkas Z, Lázár V, Györkei Á, Apjok G, Boross G, Szappanos B, Grézal G, Faragó A, Bodai L, Papp B, Pál C. 2019. Rapid decline of bacterial drug-resistance in an antibiotic-free environment through phenotypic reversion. eLife 8:e47088. https://doi.org/10.7554/ el ife 47088
- Vemuri GN, Altman E, Sangurdekar DP, Khodursky AB, Eiteman MA. 2006. Overflow metabolism in *Escherichia coli* during steady-state growth: transcriptional regulation and effect of the redox ratio. Appl Environ Microbiol 72:3653–3661. https://doi.org/10.1128/AEM.72.5.3653 -3661 2006
- Vemuri GN, Eiteman MA, Altman E. 2006. Increased recombinant protein production in *Escherichia coli* strains with overexpressed water-forming NADH oxidase and a deleted ArcA regulatory protein. Biotechnol Bioeng 94:538–542. https://doi.org/10.1002/bit.20853.
- Li L, Kromann S, Olsen JE, Svenningsen SW, Olsen RH. 2017. Insight into synergetic mechanisms of tetracycline and the selective serotonin reuptake inhibitor, sertraline, in a tetracycline-resistant strain of *Escherichia* coli. J Antibiot 70:944–953. https://doi.org/10.1038/ja.2017.78.
- Fuhrer T, Zampieri M, Sévin DC, Sauer U, Zamboni N. 2017. Genomewide landscape of gene-metabolome associations in *Escherichia coli*. Mol Syst Biol 13:907. https://doi.org/10.15252/msb.20167150.
- Kohanski MA, Dwyer DJ, Hayete B, Lawrence CA, Collins JJ. 2007. A common mechanism of cellular death induced by bactericidal antibiotics. Cell 130:797–810. https://doi.org/10.1016/j.cell.2007.06.049.
- Cokol M, Kuru N, Bicak E, Larkins-Ford J, Aldridge BB. 2017. Efficient measurement and factorization of high-order drug interactions in *Mycobacterium tuberculosis*. Sci Adv 3:e1701881. https://doi.org/10.1126/sciadv.1701881.
- Zampieri M, Enke T, Chubukov V, Ricci V, Piddock L, Sauer U. 2017. Metabolic constraints on the evolution of antibiotic resistance. Mol Syst Biol 13:917. https://doi.org/10.15252/msb.20167028.
- 78. Horinouchi T, Maeda T, Kotani H, Furusawa C. 2020. Suppression of antibiotic resistance evolution by single-gene deletion. Sci Rep 10:1–9. https://doi.org/10.1038/s41598-020-60663-6.

- Munoz-Bellido JL, Munoz-Criado S, Garcia-Rodriguez JA. 2000. Antimicrobial activity of psychotropic drugs: selective serotonin reuptake inhibitors. Int J Antimicrob Agents 14:177–180. https://doi.org/10.1016/S0924-8579(99)00154-5.
- Bohnert JA, Szymaniak-Vits M, Schuster S, Kern WV. 2011. Efflux inhibition by selective serotonin reuptake inhibitors in *Escherichia coli*. J Antimicrob Chemother 66:2057–2060. https://doi.org/10.1093/jac/dkr258.
- Peterson EJR, Ma S, Sherman DR, Baliga NS. 2016. Network analysis identifies Rv0324 and Rv0880 as regulators of bedaquiline tolerance in *Mycobacterium tuberculosis*. Nat Microbiol 1:16078. https://doi.org/10.1038/nmicrobiol.2016.78.
- 82. Brochado AR, Telzerow A, Bobonis J, Banzhaf M, Mateus A, Selkrig J, Huth E, Bassler S, Zamarreño Beas J, Zietek M, Ng N, Foerster S, Ezraty B, Py B, Barras F, Savitski MM, Bork P, Göttig S, Typas A. 2018. Species-specific activity of antibacterial drug combinations. Nature 559:259–263. https://doi.org/10.1038/s41586-018-0278-9.
- 83. Worthington RJ, Melander C. 2013. Combination approaches to combat multidrug-resistant bacteria. Trends Biotechnol 31:177–184. https://doi.org/10.1016/j.tibtech.2012.12.006.
- Weinstein ZB, Bender A, Cokol M. 2017. Prediction of synergistic drug combinations. Curr Opin Syst Biol 4:24–28. https://doi.org/10.1016/j .coisb.2017.05.005.
- 85. Levin-Reisman I, Ronin I, Gefen O, Braniss I, Shoresh N, Balaban NQ. 2017. Antibiotic tolerance facilitates the evolution of resistance. Science 355: 826–830. https://doi.org/10.1126/science.aaj2191.
- 86. Loui C, Chang AC, Lu S. 2009. Role of the ArcAB two-component system in the resistance of *Escherichia coli* to reactive oxygen stress. BMC Microbiol 9:183. https://doi.org/10.1186/1471-2180-9-183.
- Girgis HS, Hottes AK, Tavazoie S. 2009. Genetic architecture of intrinsic antibiotic susceptibility. PLoS One 4:e5629. https://doi.org/10.1371/ journal.pone.0005629.
- Cokol-Cakmak M, Bakan F, Cetiner S, Cokol M. 2018. Diagonal method to measure synergy among any number of drugs. J Vis Exp: e57713. https://doi.org/10.3791/57713.
- 89. Adolfsen KJ, Brynildsen MP. 2015. A kinetic platform to determine the fate of hydrogen peroxide in *Escherichia coli*. PLoS Comput Biol 11: e1004562. https://doi.org/10.1371/journal.pcbi.1004562.
- Baldi P, Long AD. 2001. A Bayesian framework for the analysis of microarray expression data: regularized t-test and statistical inferences of gene changes. Bioinformatics 17:509–519. https://doi.org/10.1093/bioinformatics/17.6.509.
- 91. Huang DW, Sherman BT, Lempicki RA. 2009. Systematic and integrative analysis of large gene lists using DAVID bioinformatics resources. Nat Protoc 4:44–57. https://doi.org/10.1038/nprot.2008.211.
- Peterson EJ, Bailo R, Rothchild AC, Arrieta-Ortiz ML, Kaur A, Pan M, Mai D, Abidi AA, Cooper C, Aderem A, Bhatt A, Baliga NS. 2019. Path-seq identifies an essential mycolate remodeling program for mycobacterial host adaptation. Mol Syst Biol 15:e8584. https://doi.org/10.15252/msb.20188584.
- 93. Arrieta-Ortiz ML, Hafemeister C, Shuster B, Baliga NS, Bonneau R, Eichenberger P. 2020. Inference of bacterial small RNA regulatory networks and integration with transcription factor-driven regulatory networks. mSystems 5:e00057-20. https://doi.org/10.1128/mSystems.00057-20.
- 94. Pang Z, Chong J, Zhou G, de Lima Morais DA, Chang L, Barrette M, Gauthier C, Jacques P-É, Li S, Xia J. 2021. MetaboAnalyst 5.0: narrowing the gap between raw spectra and functional insights. Nucleic Acids Res 49:W388–W396. https://doi.org/10.1093/nar/gkab382.
- 95. Bolger AM, Lohse M, Usadel B. 2014. Trimmomatic: a flexible trimmer for Illumina sequence data. Bioinformatics 30:2114–2120. https://doi.org/10.1093/bioinformatics/btu170.
- 96. Vaser R, Šikić M. 2021. Time-and memory-efficient genome assembly with Raven. Nat Comput Sci 1:332–336. https://doi.org/10.1038/s43588 -021-00073-4.
- 97. Vaser R, Sović I, Nagarajan N, Šikić M. 2017. Fast and accurate *de novo* genome assembly from long uncorrected reads. Genome Res 27:737–746. https://doi.org/10.1101/gr.214270.116.
- 98. Cawley S, Abbate E, Abraham CG, Alvarez S, Barber M, Bolte S, Bruand J, Church DM, Davis C, Estes M, Federowicz S, Fox R, Gander MW, Garst AD, Gencer G, Halweg-Edwards AL, Hardenbol P, Hraha T, Jain S, Johnson C, Juneau K, Krishnamurthy N, Lambert S, Leland B, Pearson F, Ray JCJ, Sanada CD, Shaver TM, Shepherd TR, Shorenstein J, Spindler EC, Struble CA, Swat MH, Tanner S, Tian T, Wishart K, Graige MS. 2021. A framework for evaluating edited cell libraries created by massively parallel genome engineering. bioRxiv. https://doi.org/10.1101/2021.09.23.458228.

- Fernandes AD, Macklaim JM, Linn TG, Reid G, Gloor GB. 2013. ANOVAlike differential expression (ALDEx) analysis for mixed population RNA-Seq. PLoS One 8:e67019. https://doi.org/10.1371/journal.pone.0067019.
- 100. Boehme M, Guzzetta KE, Bastiaanssen TFS, van de Wouw M, Moloney GM, Gual-Grau A, Spichak S, Olavarría-Ramírez L, Fitzgerald P, Morillas E, Ritz NL, Jaggar M, Cowan CSM, Crispie F, Donoso F, Halitzki E, Neto MC, Sichetti M, Golubeva AV, Fitzgerald RS, Claesson MJ, Cotter PD, O'Leary OF, Dinan TG, Cryan JF. 2021. Microbiota from young mice counteracts selective age-associated behavioral deficits. Nat Aging 1:666–676. https://doi.org/10.1038/s43587-021-00093-9.
- 101. R Core Team. 2021. R: A language and environment for statistical computing. R foundation for statistical computing, Vienna, Austria.
- 102. Keseler IM, Mackie A, Santos-Zavaleta A, Billington R, Bonavides-Martínez C, Caspi R, Fulcher C, Gama-Castro S, Kothari A, Krummenacker M, Latendresse M, Muñiz-Rascado L, Ong Q, Paley S, Peralta-Gil M,

- Subhraveti P, Velázquez-Ramírez DA, Weaver D, Collado-Vides J, Paulsen I, Karp PD. 2017. The EcoCyc database: reflecting new knowledge about *Escherichia coli* K-12. Nucleic Acids Res 45:D543–D550. https://doi.org/10.1093/nar/qkw1003.
- Orth JD, Conrad TM, Na J, Lerman JA, Nam H, Feist AM, Palsson BØ. 2011. A comprehensive genome-scale reconstruction of *Escherichia coli* metabolism—2011. Mol Syst Biol 7:535. https://doi.org/10.1038/msb.2011.65.
- 104. Unden G, Bongaerts J. 1997. Alternative respiratory pathways of *Escherichia coli*: energetics and transcriptional regulation in response to electron acceptors. Biochim Biophys Acta 1320:217–234. https://doi.org/10.1016/s0005-2728(97)00034-0.
- 105. Shannon P, Markiel A, Ozier O, Baliga NS, Wang JT, Ramage D, Amin N, Schwikowski B, Ideker T. 2003. Cytoscape: a software environment for integrated models of biomolecular interaction networks. Genome Res 13:2498–2504. https://doi.org/10.1101/gr.1239303.